Unravelling Genomic Signatures of lncRNA Expression in Zebrafish Caudal Fin Regeneration: Bridging Regenerative Potential and Positional Memory

Soumyadeep Paul , A Hariharan , Dasari Abhilash , Surbhi Kohli , Shilpi Minocha * , Ishaan Gupta *

Posted Date: 21 April 2026

doi: 10.20944/preprints202604.1402.v1

Keywords: zebrafish; fin regeneration; positional memory; long non-coding RNAs; bulk-RNA sequencing analysis; core stress response

 doi:10.20944/preprints202604.1402.v1

Article

Unravelling Genomic Signatures of lncRNA Expression in Zebrafish Caudal Fin Regeneration: Bridging Regenerative Potential and Positional Memory

Soumyadeep Paul [1], A Hariharan [2], Dasari Abhilash [1], Surbhi Kohli [1], Shilpi Minocha [2,*] and Ishaan Gupta [1,*]

[1] Department of Biochemical Engineering and Biotechnology, Indian Institute of Technology, Delhi

[2] Kusuma School of Biological Sciences, Indian Institute of Technology, Delhi

* Correspondence: shilpi.minocha@bioschool.iitd.ac.in (S.M.); ishaan.gupta@dbeb.iitd.ac.in (I.G.)

Abstract

Using zebrafish as a model, we characterized novel long non-coding RNAs linked to caudal fin regeneration and positional memory, uncovering evolutionarily conserved candidates with potential cross-species relevance. RNA-seq data deposited in the NCBI database were compared at various important time points (0h post-amputation (hpa), 12 hpa, 1 day post-amputation (dpa), two dpa, three dpa, and seven dpa) and fin parts (proximal, middle, and distal) to uncover major regulatory lncRNAs. Using HISAT2, StringTie, FEELnc, Conservation Analysis, and WGCNA, our analysis revealed 107 lncRNAs associated with specific regeneration time points and 229 lncRNAs involved in positional memory during the regenerative process. We identified 13 common genomic regions that are complete or partial lncRNAs, indicating a functional connection between regeneration and positional identity, and expressed differently at each time point and each position. Additionally, a comparison with regeneration-associated mRNAs revealed that these 13 regions play critical roles in both processes, providing insights into the molecular mechanisms of regenerative precision. RT-PCR validation confirmed position-specific differential expressions of these overlapping regions despite identical injury, suggesting roles in regenerative regulation and evolutionary adaptation.

Keywords: zebrafish; fin regeneration; positional memory; long non-coding RNAs; bulk-RNA sequencing analysis; core stress response

1. Introduction

Long non-coding RNAs (lncRNAs) are RNA molecules greater than 200 nucleotides in length that do not code for proteins, but they help control gene activity and support many important functions inside the cell. In biological systems, lncRNAs act as master regulators of the genome, regulating transcription, post-transcriptional processes, and chromatin remodelling [1]. Their roles in early embryogenesis, pluripotency induction, and germ cell formation make them important in a developmental biology context [2]. LncRNAs regulate gene expression at multiple levels, including chromatin modulation, thereby orchestrating embryonic development, cell fate decisions, and complex biological processes, making them key targets for understanding and manipulating development [3].

Non-coding RNAs have been recognized as important players in regulating tissue regeneration, coordinating intricate molecular events that indicate regeneration and renewal [4]. LncRNAs play important roles in the different phases of regeneration, from triggering the healing response to directing tissue remodelling, by binding to mRNAs, microRNAs, and proteins [5]. Their dynamic expression in the various phases of regeneration emphasizes their role in coordinating the

 doi:10.20944/preprints202604.1402.v1

regenerative process [6]. LncRNAs have also been shown to regulate regenerative processes, including cellular senescence, stem cell pluripotency, and differentiation, thereby positioning them at the centre of the regenerative story [7]. Recent investigations have identified lncRNAs' role in transcending cellular senescence, with therapeutic potential in avoiding age-related diseases and enhancing tissue regeneration [4]. By regulating gene programs that control tissue repair, lncRNAs may represent promising therapeutic targets for enhancing healing and treating age-associated diseases. [8].

The identification of universal lncRNAs promoting regeneration across species remains a critical challenge in the field, hindered by their rapid evolution and species-specific functionality [9]. The recently developed RegenDbase addresses this by documenting lncRNAs involved in regeneration across organisms like zebrafish, axolotl, and mouse, providing insights into their regulatory control on evolutionarily conserved regeneration pathways [10]. However, significant hurdles persist in identifying well-defined regions within the non-coding genome that universally promote or regulate regeneration across species, a limitation that highlights a crucial avenue for future research [9]. The complexity of lncRNA functions, coupled with technological and methodological limitations, further complicates this identification process [11]. Addressing these challenges requires advancements in technology and methodology, as well as a more comprehensive understanding of lncRNA conservation and function across species [9]. The continued development of resources like RegenDbase, combined with cross-species analysis and innovative approaches to evaluate lncRNA conservation, holds promise for unravelling the complex regulatory networks governing tissue regeneration, potentially leading to breakthroughs in regenerative medicine [10].

The ability of human cells to regenerate differs profoundly between organs, with the liver having an outstanding capacity to regenerate through hepatocyte division and stem cell activation, while the heart exhibits limited regenerative capacity due to the loss of cardiomyocyte proliferative capacity during early development. This extreme difference in the capacity of organs to regenerate poses both challenges and opportunities for the design of site-specific therapeutic approaches in regenerative medicine. In such a scenario, using a model organism to understand the pathways and mechanisms underlying regeneration can be quite useful.

Zebrafish have become a prominent model organism for regeneration research due to their remarkable ability to regenerate various tissues, including fins, heart, and brain. They offer unique advantages for studying lncRNA-mediated regeneration. [12]. This model system has provided valuable insights into the molecular mechanisms underlying tissue repair and regeneration, with studies identifying hundreds of differentially expressed lncRNAs during cardiac and fin regeneration processes [13], offering valuable insights with potential translational applications to human medicine. These fish share approximately 70% of their genes with humans, including 84% of disease-associated genes, making them highly relevant for biomedical research [14]. Recent studies have revealed hundreds of differentially expressed lncRNAs during zebrafish brain regeneration [15]. The remarkable regenerative abilities of zebrafish, coupled with their genetic similarity to humans, have made them invaluable for modelling human diseases and understanding tissue regeneration mechanisms, particularly in cardiovascular diseases, renal regeneration, and cancer research [16]. This research not only elucidates the molecular mechanisms underlying regeneration but also offers promising avenues for developing new therapeutic strategies in human regenerative medicine.

Previous studies have laid a strong foundation for understanding the molecular mechanisms underlying fin regeneration. For instance, research identified 489 genes with differential expression between proximal and distal regenerating tissues, including 29 genes with proximal enrichment and 460 with distal enrichment [17]. This spatial regulation of gene expression during regeneration highlights the potential for lncRNAs to play crucial roles in maintaining positional information and guiding the regeneration process. The position-dependent nature of fin regeneration is exemplified by the formation of joints in regenerating fins. The expression of genes such as evx1, dlx5a, and mmp9 is crucial for joint formation and is influenced by the positional context within the fin [18]. This

 doi:10.20944/preprints202604.1402.v1

demonstrates how the location of cells within the fin can significantly affect the regeneration process and outcome.

Furthermore, the study of chromatin modifications during fin regeneration has revealed that H3K4me3 levels increase over gene promoters that become transcriptionally active, recapitulating patterns observed during embryonic development [19]. This suggests that regeneration may involve the reactivation of developmental programs, which could be regulated by lncRNAs in a position-specific manner. The study of lncRNAs in zebrafish fin regeneration, with its distinct positional memory and spatially regulated gene expression, offers a unique opportunity to unravel the complex regulatory networks governing tissue regeneration.

Firstly, this study uses the best available transcriptome-wide approaches to identify and characterize novel lncRNAs involved in zebrafish caudal fin regeneration. Integrating RNA-seq data analysis using powerful computational tools with validation through an experimental approach may enable the provision of a complete map of the time-course landscape of lncRNA expression. Our focus is on key time points corresponding to well-defined stages of regeneration: the wound-healing phase (0-12 hours post-amputation), the blastema-formation phase (1-2 days post-amputation), and the regenerative outgrowth phase (3-7 days post-amputation).

Secondly, this study aims to further our understanding of the molecular basis of positional memory in zebrafish caudal fin regeneration by analyzing RNA sequencing data to identify and characterize novel lncRNAs associated with spatial identity. By employing advanced bioinformatics tools and statistical analyses, we aim to uncover distinct lncRNA expression patterns along the proximodistal axis and their potential roles in guiding regeneration. Our findings may provide new avenues for therapeutic interventions in regenerative medicine, potentially leading to improved strategies for tissue repair and regeneration in humans [20,21].

2. Results

2.1. Genome-Wide Discovery and Analysis of Novel lncRNAs in Zebrafish Caudal Fin Regeneration

The RNA sequencing data, sourced from the NCBI database, consisted of 6 samples collected at various time points following caudal fin amputation in zebrafish. These time points included 0 hours post-amputation (hpa), 12 hpa, 1 day post-amputation (dpa), 2 dpa, 3 dpa, and 7 dpa, corresponding to different stages of the regeneration process. Transcriptome-wide profiling enabled the systematic discovery of novel lncRNAs expressed during regeneration. Dynamic expression patterns were observed, reflecting stage-specific regulation of lncRNA networks. Early time points were enriched for lncRNAs associated with immune and wound responses, whereas intermediate and later stages showed induction of lncRNAs linked to blastema proliferation, extracellular matrix organization, and skeletal patterning. This genome-wide catalogue of regeneration-associated lncRNAs establishes a framework for exploring their putative roles in coordinating the molecular transitions from wound closure to blastema-driven regrowth and tissue remodelling.

Transcriptome Assembly and Mapping:

The initial quality assessment of our raw sequencing data, performed using FastQC, revealed high-quality metrics across all samples, with an average Phred score of more than 30. After trimming adapters and low-quality bases using Trimmomatic, the cleaned data were aligned to the zebrafish reference genome (GRCz11) using HISAT2. This alignment achieved a high mapping efficiency, with an average of 92% of reads successfully aligned. Transcriptome assembly was carried out using StringTie, which integrated the alignments and identified approximately 892,910 transcripts, including both known and novel isoforms.

Identification of potential LncRNA candidates:

Utilizing the FEELnc pipeline, we classified transcripts from our de novo transcriptome assembly into coding (mRNAs) and long non-coding RNAs (lncRNAs). FEELnc identified 10,113 putative lncRNAs based on coding potential, multi-k-mer profiles, and constrained open reading frame (ORF) characteristics. To investigate their evolutionary trajectory, we employed PhastCons, a

 doi:10.20944/preprints202604.1402.v1

phylogenetic hidden Markov model that integrates multiple vertebrate genomes, to quantify conservation. Since lncRNAs exhibit low conservation across different species, it was assumed that lncRNAs with any degree of conservation may harbor pivotal biological functions. Therefore, we specifically focused on the 6,114 lncRNAs that manifested non-zero conservation. We further refined this subset to those with at least 50% overlap within conserved regions and ultimately isolated the top 5% based on conservation metrics Supplementary Document 1. This approach yielded 1,514 lncRNAs, having pronounced conservation signatures. These highly conserved lncRNAs, therefore, could emerge as prime candidates for downstream functional characterization, as their evolutionary preservation suggests potential biological relevance.

We assessed the expression profiles of identified lncRNA candidates across various samples using principal component analysis (PCA) of normalized lncRNA counts (Figure 1A) and a heatmap of lncRNAs expression (Figure 1B). The PCA results showed that samples from 1-day post-lesion (1dpl) distinctly clustered apart from other stages, which were closer to 12hpa. This shows that novel lncRNAs are highly active immediately after injury and gradually decline during recovery. This pattern was corroborated by a sample-to-sample distance heatmap, which shows lower correlations (blue) between 72 hrs and other time points, suggesting divergence in expression patterns at this stage. These observations suggest that the expression of these lncRNAs is particularly altered during the initial stage of wound healing, possibly playing critical roles in the initial stage of brain regeneration, after which regeneration continues. Similar pattern of lncRNAs being active during early injury, while their pattern reduces during late stages in traumatic brain injury in zebrafish [15].

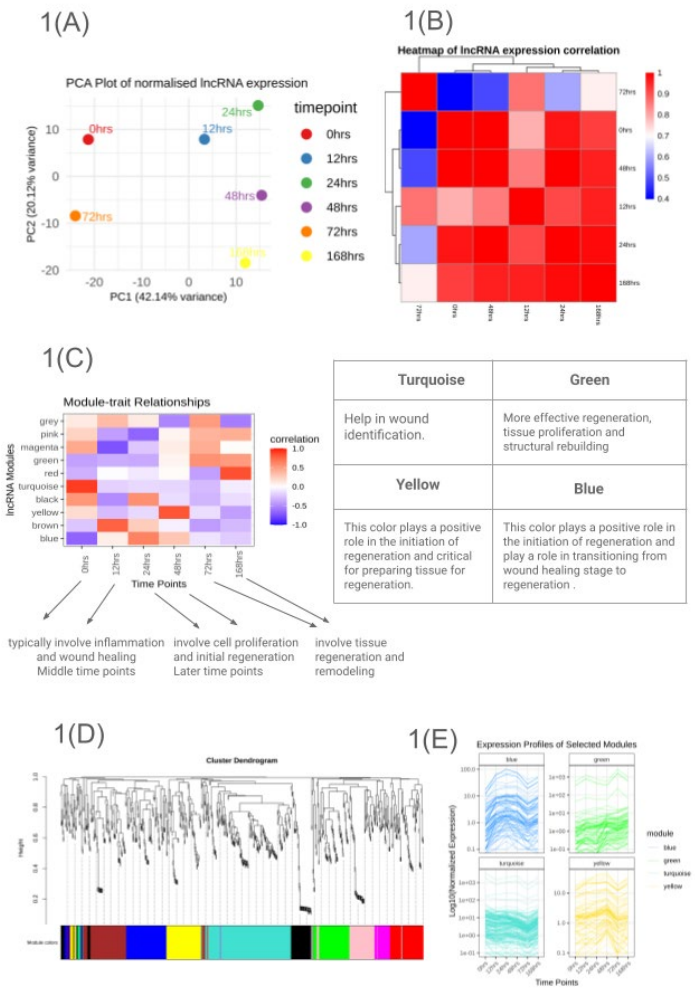

Figure 1. (A) PCA plot of normalized lncRNA expression. (B) Heatmap of lncRNA expression correlation between samples. This heatmap provides insights into how lncRNA expression changes over time, highlighting

 doi:10.20944/preprints202604.1402.v1

periods of similarity and divergence in expression profiles. (C) Heatmap showing the correlation of expression profiles among lncRNA clusters. Turquoise, Green, Yellow, and Blue modules show some significant changes. (D) Dendrogram of WGCNA Clusters with 15,14 novel lncRNA. (E) Expression profiles of the individual long non-coding RNAs in the selected modules co-expressed cluster. The Y-axis indicates normalized gene expression, and the X-axis indicates samples labelled according to the treatment.

We performed Weighted Gene Co-expression Network Analysis (WGCNA) to pinpoint clusters of highly co-expressed novel lncRNAs with distinct sample-specific expression patterns (Figure 1B). This approach aimed to identify novel lncRNAs that may regulate fin regeneration. Our analysis identified 10 modules with unique expression profiles across the fin injury recovery timeline (Figure 1C and 1D). We filter the module after seeing their expression profile (Figure 1E) and find 4 modules are important as per our biological question, which are turquoise, green, blue and yellow.

We identified 183 novel lncRNAs in the turquoise module, 79 in the green module, 102 in the blue module, and 85 in the yellow module. To ensure the accuracy of our functional inference, we implemented stringent criteria, excluding any novel lncRNAs located within 2.5 kb of coding genes to avoid potential interference with genes. This filtration left us with 46 lncRNAs in the turquoise module, 20 in the green module, 23 in the blue module, and 18 in the yellow module.

Table 1. Gene proximity analysis filtering table.

MODULE	Gene before proximity Filtering	Gene after proximity Filtering	Transcript before proximity Filtering	Transcript after Proximity Filtering
TURQUOISE	**120**	**33**	**183**	**46**
GREEN	**61**	**16**	**79**	**20**
BLUE	**77**	**17**	**102**	**23**
YELLOW	**56**	**13**	**85**	**18**

Functional significance of identified lncRNAs:

To further elucidate the biological relevance of these newly identified lncRNAs, we extended our analysis by correlating their expression profiles with those of established protein-coding genes. We prioritized genes exhibiting a robust correlation ($|r| > 0.9$) with the lncRNAs and subsequently performed Gene Ontology (GO) and KEGG pathway enrichment analyses. This approach aimed to uncover the biological processes and pathways potentially modulated by these lncRNAs during the early wound-healing phase of brain regeneration. Notably, genes co-expressed with lncRNAs in the brown module were enriched for metabolic pathways pertinent to RNA splicing and peptide biosynthetic processes. This suggests that these lncRNAs may be pivotal in orchestrating these foundational cellular activities (Figure 2).

These modules exhibited unique expression signatures, each playing a critical role in fin regeneration. Pathway enrichment analysis indicated that lncRNAs in the blue module govern the BMP signalling pathway, ribosome biogenesis, and cellular responses to growth factor stimuli. Turquoise module lncRNAs were enriched in the Wnt signalling pathway and cell projection morphogenesis. The yellow module was linked to DNA damage response, double-strand break repair, and DNA recombination pathways. Finally, lncRNAs within the green module were implicated in the metabolic processes of organic hydroxy compounds.

 doi:10.20944/preprints202604.1402.v1

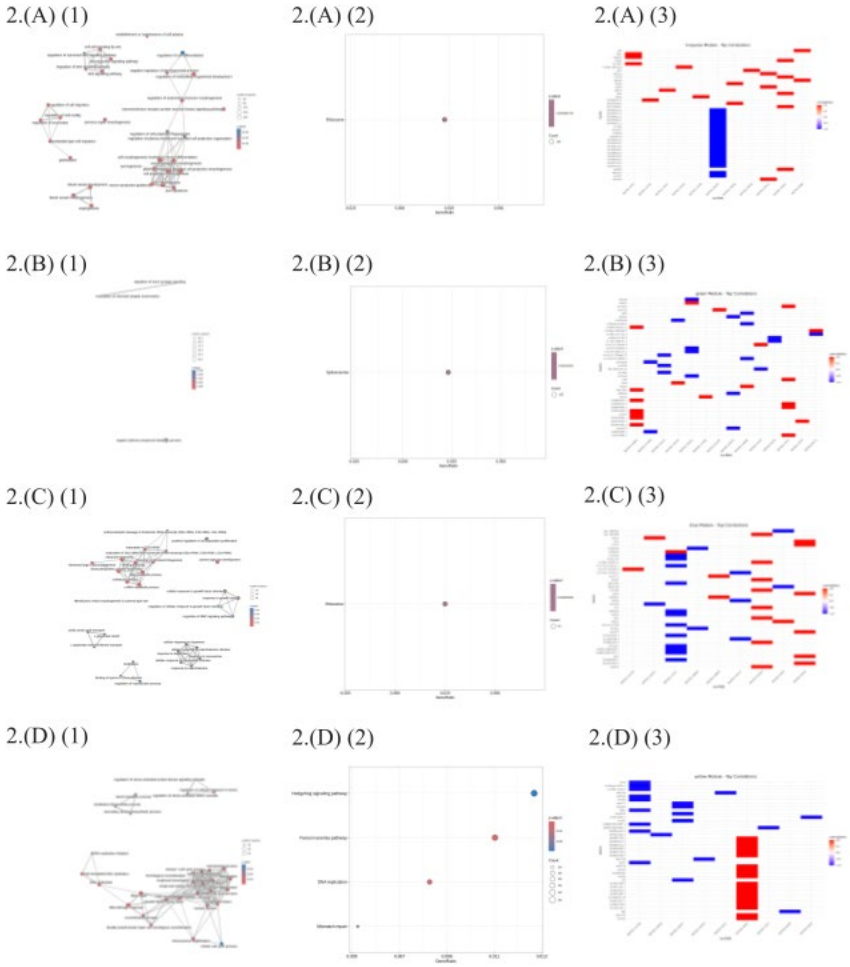

Figure 2. Functional enrichment analysis of gene modules correlated with long non-coding RNAs (lncRNAs). Panels (A) to (D) correspond to the turquoise, green, blue, and yellow modules, respectively. For each module: (1) EMAP plot showing GO enrichment of biological processes for genes with a 90% correlation in expression with lncRNAs, (2) Dot plot of KEGG pathway enrichment analysis for genes highly correlated (r > 0.90) with lncRNAs; (3) The highest and lowest 20 correlation genes with novel lncRNAs. These visualizations highlight the key biological functions and pathways associated with each long non-coding RNA (lncRNA) co-expression module.

Blue Module: BMP Signalling, Ribosome Biogenesis, and Growth Factor Responses

The blue module includes key processes involved in fin regeneration, such as BMP signalling, ribosome biogenesis, and growth factor responses (Figure 2C). Bone Morphogenetic Proteins (BMPs), members of the TGF-β superfamily, play an essential role in regulating growth and differentiation during zebrafish fin regeneration. [22][23]. MYC-driven ribosome biogenesis supports increased protein synthesis during regeneration, facilitating tissue regrowth and differentiation. Together with TGF-β–related pathways, these mechanisms coordinate cell proliferation, differentiation, and survival during fin repair and regeneration. [24].

MSTRG.24019.1 exhibits strong positive correlations with three genes involved in regenerative processes. Illr1 (Interleukin-1 Receptor Like 1), correlated at (0.9947124), is necessary for immune responses that support tissue repair [25]. aldocb, exhibiting a correlation of (0.9940187), is involved in tissue regeneration [26]. Finally, zgc:101699 (Zebrafish Gene Collection clone 101699) correlates at (0.9921206) and is known to be involved in both regenerative processes and regenerative signalling [27]. These associations point to a potential role for MSTRG.24019.1 in coordinating immune-mediated and molecular mechanisms vital to effective regeneration.

 doi:10.20944/preprints202604.1402.v1

Turquoise Module: Wnt Signalling and Cell Projection Morphogenesis

Wnt/β-catenin signalling is a key regulator of zebrafish fin regeneration, controlling organising centres that direct tissue growth and patterning. [28] (Figure 2A). Notably, Wnt signalling is active primarily in the no proliferative distal blastema, suggesting that it regulates fin regeneration indirectly via secondary signalling cues. [29]. The pathway's influence extends to epidermal patterning and osteoblast differentiation, highlighting its role in bone regeneration within the fin [29]. Both canonical and non-canonical Wnt pathways contribute to regeneration across species, including zebrafish, and regulate cell projection morphogenesis, which is essential for proper cellular alignment and tissue integration during regeneration [30]; [28].

MSTRG.1053.1 exhibits significant correlations with three key genes, soga3a, tfpi2, and slc10a1, participating in regenerative processes and tissue maintenance. Soga3a, which shows the strongest correlation (0.9992015), is involved in regenerative processes and contributes to the cellular response to stress [31]. Tfpi2 (0.9965104) plays a critical part in tissue remodelling, including wound healing and regeneration [32]. Similarly, slc10a1 (0.9954736) is linked to cellular homeostasis and supports regenerative responses [33]. These associations underline the importance of MSTRG.1053.1 in pathways involved in cellular repair, regeneration, and general tissue health.

Yellow Module: DNA Damage Response and Repair

lncRNAs in the yellow module are linked to DDR, DSB repair, and DNA recombination pathways, including homologous recombination (HR) and non-homologous end joining (NHEJ), which maintain genomic stability during rapid fin regeneration (Figure 2D). [34,35]. Recent studies show particle radiation affects DNA end processing and repair, processes crucial for maintaining cell function and enabling regeneration [36]. While specific studies on fin regeneration were not directly cited, the general importance of these pathways in regeneration is supported by their role in cellular recovery and tissue regeneration across various species [37].

MSTRG.6825.1 is significantly correlated with three genes of critical importance for regeneration and cellular homeostasis. Specifically, it is significantly negatively correlated (-1) with acanb (actin-related protein), which is key in tissue remodelling, regeneration, and cytoskeleton organization, and adcy1b (adenylate cyclase 1b), an enzyme participating in signal transduction and playing a crucial role in regenerative processes [38]. Further, MSTRG.6825.1 shows a correlation with asb10 (Ankyrin repeat and SOCS box containing 10), which is involved in protein degradation pathways, maintenance of protein homeostasis, and stress responses during regeneration [39]. Together, these correlations suggest the possible involvement of MSTRG.6825.1 in regulating regenerative pathways and maintaining cellular balance.

Green Module: Metabolic Processes of Organic Hydroxy Compounds

The green module implicates lncRNAs in the metabolic processes of organic hydroxy compounds, which play significant roles in cellular metabolism and signalling pathways crucial for tissue regeneration [40] (Figure 2B). Organic hydroxy compounds support biomolecule synthesis and modification, while the TCA cycle supplies energy and biosynthetic precursors essential for regeneration. [41]. Selective steroid hydroxylation and related metabolic pathways provide essential biochemical regulation, energy, and building blocks required for cell proliferation and differentiation during fin regeneration. [42].

Three critical genes involved in regeneration have marked negative correlations with MSTRG.15167.2. Nme2a (Nucleoside Diphosphate Kinase 2a), with a correlation of (-0.9938864), plays a central role in cell proliferation and regenerative processes [43]. Lrrc4ba (Leucine Rich Repeat Containing 4Ba), with a correlation of (-0.9902127), is important to neural regeneration; hence, this might suggest MSTRG.15167 plays a role in nervous system repair [44]. In addition, si:ch211-238p8.31 (correlation is -0.9897972) is a zebrafish-specific gene reported to be involved in tissue regeneration [45]. Overall, the negative correlations suggest a possible regulatory function of MSTRG.15167.2 across different regenerative pathways.

 doi:10.20944/preprints202604.1402.v1

2.2. Genome-Wide Discovery and Analysis of Novel lncRNAs in Zebrafish Fins, Revealing Positional Memory

The RNA sequencing data, sourced from the Gene Expression Omnibus (GEO) database (accession no. GSE92760), consisted of 14 samples (we failed to download the SRR5125781_Mid_4 data) collected from three distinct regions along the proximodistal axis of the zebrafish caudal fin: proximal, middle, and distal. Each region was represented by five biological replicates, with each replicate comprising pooled fin tissue from two male and two female zebrafish. This dataset captures the spatially regulated transcriptomic landscape of the caudal fin, providing insights into the molecular basis of positional memory.

The proximal region is characterized by gene expression patterns associated with enhanced regenerative capacity, whereas the distal region exhibits gene expression signatures linked to positional identity maintenance. The middle region serves as a transitional zone, reflecting a mix of both proximal and distal transcriptomic signatures. Notably, lncRNAs emerge as key regulators in defining positional identity, contributing to spatially coordinated regenerative processes. This classification allows for a comprehensive investigation of the molecular mechanisms underlying positional memory and the spatially distinct regulatory networks that drive zebrafish caudal fin regeneration.

Transcriptome Assembly and Mapping:

FastQC showed high-quality sequencing data (Phred >30). After trimming with Trimmomatic, HISAT2 achieved ~94% mapping to the zebrafish genome (GRCz11). StringTie assembly identified 975,355 transcripts (known and novel), of which 973,078 were retained after removing unplaced scaffolds.

Identification of potential LncRNA candidates:

Using FEELnc, we identified 23,778 putative lncRNAs, of which 10,040 showed non-zero conservation. By selecting transcripts with at least 50% overlap in conserved regions and isolating the top 5% based on conservation metrics, we obtained 3,352 highly conserved lncRNAs, making them strong candidates for functional relevance. PCA of their expression across proximal, middle, and distal fin regions showed that distal samples clustered separately from proximal and middle regions, suggesting a distinct transcriptomic identity and reinforcing the role of lncRNAs in maintaining positional memory during regeneration (Figure 3A).

This pattern was further supported by a sample-to-sample distance heatmap (Figure 3B), which showed lower correlations (blue) between the distal region and the other two regions, highlighting its distinct gene expression landscape. These observations suggest that lncRNAs are particularly crucial in defining the positional identity of the distal region, potentially regulating region-specific regenerative processes in zebrafish caudal fin regeneration. Weighted Gene Co-expression Network Analysis (WGCNA) identified 6 modules with unique expression profiles across the fin injury recovery timeline. (Figure 3C and 3D). We filter the module after seeing there expression profile (Figure 3E) and find 4 modules are important as per our biological question which are turquoise, brown, blue and yellow.

 doi:10.20944/preprints202604.1402.v1

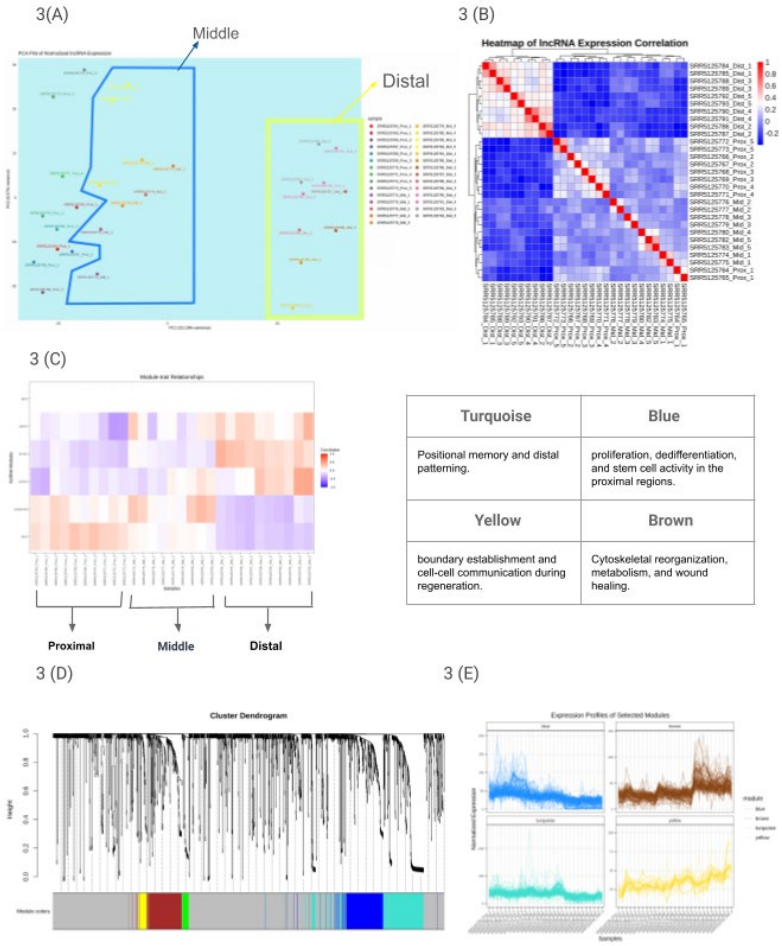

Figure 3. (A) PCA plot of normalized lncRNA expression. (B) Heatmap of lncRNA expression correlation between all samples. (C) Heatmap illustrating the correlation of expression profiles among long non-coding RNA (lncRNA) clusters. Turquoise, Brown, Yellow, and Blue modules show some significant changes. (D) Dendrogram of WGCNA Clusters with 3,352 novel lncRNAs. (E) Expression profiles of the individual long non-coding RNAs in the selected modules co-expressed cluster. The Y-axis indicates normalized gene expression, and the X-axis indicates samples labeled according to the treatment.

Among these modules, 136 novel lncRNA genes were present in the turquoise module, 138 in the blue module, 24 in the yellow module, and 126 in the brown module. Further filtration based on the presence of genes within 2.5 kb of upstream and downstream, with 58 lncRNAs in the turquoise module, 60 in the blue module, 5 in the yellow module, and 57 in the brown module. We further analysed the expression correlations between these lncRNAs and mRNAs and filtered those with r>0.7. The yellow and blue modules failed to correlate with at least 70% correlation in the pathway enrichment process.

Table 2. Gene proximity analysis filtering table.

MODULE	Gene before proximity Filtering	Gene after proximity Filtering	Transcript before proximity Filtering	Transcript after Proximity Filtering
TURQUOISE	**136**	**58**	**271**	**149**
BROWN	**126**	**57**	**183**	**79**

 doi:10.20944/preprints202604.1402.v1

Gene ontology and pathway enrichment results revealed that lncRNA from the brown module showed enrichment for lysosome activity, autophagy, and focal adhesion pathways, suggesting its involvement in cellular remodelling, waste clearance, and spatial regulation during regeneration. In contrast, lncRNAs of the turquoise module were associated with extracellular matrix (ECM) organization, collagen metabolic processes, and bone morphogenesis, highlighting its role in maintaining axial patterning and structural integrity.

These findings indicate that the molecular coordination of positional identity is essential for guiding precise tissue restoration. By regulating distinct biological processes, the brown and turquoise modules collectively shape the regenerative landscape, ensuring the accurate reconstruction of fin architecture and function across different proximodistal segments. (Figure 4).

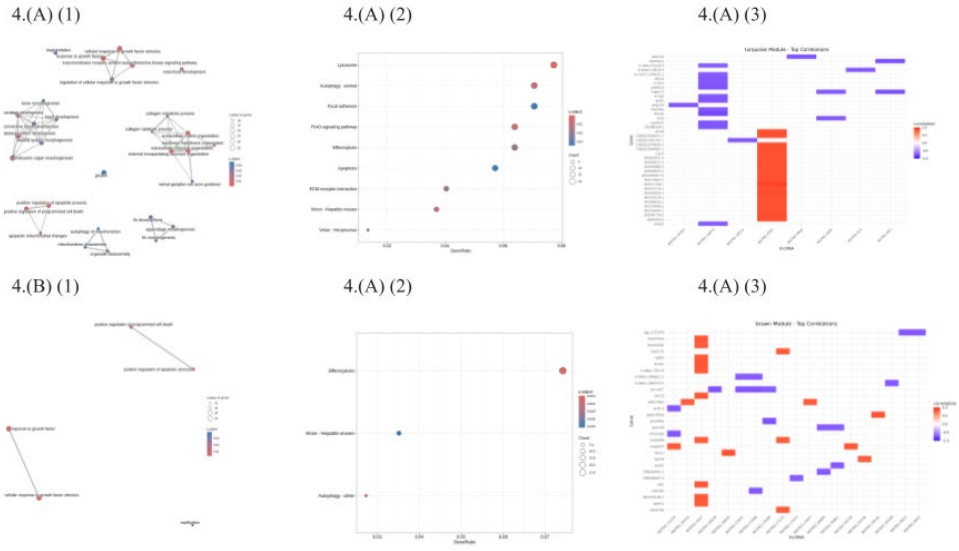

Figure 4. Functional enrichment analysis of gene modules highly correlated with long non-coding RNAs (lncRNAs). Panels (A) and (B) show the turquoise and brown modules, respectively. Each panel includes: (1) an EMAP plot depicting Gene Ontology biological processes enriched among genes with expression correlation above 0.70 with lncRNAs; (2) a Dot plot illustrating KEGG pathway enrichment for these highly correlated genes; (3) a list of the top 20 genes with the highest and lowest correlation to novel lncRNAs within each module. These representations offer insights into the biological functions and pathways associated with the identified long non-coding RNA (lncRNA) modules.

The Brown Module: Regulator of Cellular Remodelling and Positional Memory in Regeneration

The brown module is significantly enriched in pathways related to lysosome activity, autophagy, and focal adhesion, all of which play essential roles in cellular remodelling, waste clearance, and spatial regulation during regeneration [46,47] (Figure 4B). Lysosomes act as metabolic regulators, facilitating the degradation and recycling of cellular waste, which is crucial for maintaining tissue integrity [48]. Autophagy, a tightly regulated process that directs cytoplasmic material to lysosomes for degradation, ensures cellular quality control by eliminating dysfunctional organelles and proteins, thereby supporting regeneration [49]. Additionally, focal adhesion pathways mediate cell-ECM interactions, enabling structural stability and communication necessary for tissue reorganization [50]. The interplay between these processes reinforces positional memory, ensuring regenerating cells retain spatial identity by clearing damaged components and restoring their original functions [46]. Collectively, the brown module orchestrates these pathways to facilitate effective tissue repair while maintaining spatial organization essential for precise regeneration.

Analyzing the genes correlated with MSTRG.1617.1 in the brown module, we identified three key genes showing strong positive correlations that are crucial for regeneration and positional

 doi:10.20944/preprints202604.1402.v1

memory: STRIP1 (Striatin Interacting Protein 1) which plays a vital role in cell polarity and cytoskeletal organization essential for positional memory [51], TAF10 (TATA-Box Binding Protein Associated Factor 10,) which regulates transcriptional processes during regeneration and helps maintain cell identity [52] and TMEM 54A (Transmembrane Protein 54A) This lncRNA is involved in membrane organization and cellular patterning, suggesting a role in coordinating spatial organization and transcriptional regulation during regeneration and positional memory maintenance.

The Turquoise Module: ECM Organization and Structural Integrity in Regeneration

The turquoise module is enriched for ECM organization, collagen metabolism, and bone morphogenesis, providing structural and biochemical support essential for tissue repair and regeneration. [53] (Figure 4A). Collagen metabolism is fundamental to ECM stability, influencing cell adhesion, migration, and differentiation, which are critical for regeneration [54]. Bone morphogenesis pathways regulate skeletal patterning and repair by modulating osteogenic signals essential for structural reformation [55]. Together, these processes underscore the turquoise module's role in coordinating spatially regulated fin regeneration and restoring tissue architecture.

Analyzing the genes correlated with MSTRG.18674.1 in the turquoise module, we identified three key genes showing strong negative correlations that are crucial for regeneration and positional memory: PHLDB2A (Pleckstrin Homology Like Domain Family B Member 2, the correlation ~ (-0.8)) [56] which is involved in membrane targeting and signaling pathways, GRIP1 (Glutamate Receptor Interacting Protein 1, the correlation ~ (-0.75)) which plays a role in the synaptic organization and cellular positioning [57], and FBXW4 (F-Box And WD Repeat Domain Containing protein, correlation ~ (-0.75)) These findings suggest that this lncRNA may function as a negative regulator, coordinating membrane dynamics, cellular positioning, and protein degradation required for tissue remodelling and maintenance of positional memory during regeneration. [58].

List of Novel lncRNAs:

The list is given in Supplementary Document 2 for fin regeneration, Supplementary Document 3 for positional memory; only two modules of lncRNAs (brown and Turquoise) are included in positional memory.

2.3. Overlapping lncRNAs are Crucial to Both Biological Processes

We identified 107 lncRNAs involved in regeneration and 228 lncRNAs associated with positional memory. The regeneration dataset formed four modules: 23 lncRNAs in blue, 46 in turquoise, 18 in yellow, and 20 in green, while positional memory had two modules: 149 lncRNAs in turquoise and 79 in brown (Figure 5A and 5B). Several overlaps were observed, with 5 lncRNAs from the regeneration blue module overlapping with 4 in the positional memory turquoise module, 8 from the regeneration turquoise module overlapping with 68 in positional memory turquoise, 6 from regeneration turquoise overlapping with 8 in positional memory brown, and 3 from regeneration yellow overlapping with 3 in positional memory brown. The list of overlapping lncRNAs is provided in Supplementary Document 4. After analyzing their positions and identifying the most common regions, we identified 13 key regions where either the full or partial sequence of lncRNA plays a significant role in both regeneration and positional memory. These findings offer valuable insights into their potential regulatory functions and their contribution to tissue regeneration and spatial identity.

Table 3. The most important overlapping region among all lncRNAs, which is important in both biological processes.

CHR	Start Position	Stop Position	STRAND	NAME
1	59386284	59389365	+	ZEB_RE_POS_FIN_1
1	40651504	40659496	-	ZEB_RE_POS_FIN_2
1	52379492	52380379	-	ZEB_RE_POS_FIN_3
2	18334246	18335688	+	ZEB_RE_POS_FIN_4

 doi:10.20944/preprints202604.1402.v1

3	7463694	7479910	+	ZEB_RE_POS_FIN_5
4	47597472	47599262	+	ZEB_RE_POS_FIN_6
4	62329752	62330888	+	ZEB_RE_POS_FIN_7
5	11497931	11500894	+	ZEB_RE_POS_FIN_8
7	32321510	32321813	-	ZEB_RE_POS_FIN_9
16	54377947	54378474	+	ZEB_RE_POS_FIN_10
18	23459613	23461429	+	ZEB_RE_POS_FIN_11
19	19458863	19461118	-	ZEB_RE_POS_FIN_12
23	5048681	5052895	-	ZEB_RE_POS_FIN_13

The spatiotemporal expression dynamics of the 13 selected lncRNAs are illustrated in Figure 5. Figure 5(C) displays the expression variation of each lncRNA across different regeneration time points, highlighting temporal changes in transcriptional activity during the regenerative process. Figure 5(D) shows the positional expression differences of the same lncRNAs across the proximal, median, and distal regions of the regenerating fin, emphasizing their region-specific regulation. A more detailed, integrative analysis is presented in Supplementary Document 5, where BAM files from various time points were merged with those from the positional memory dataset and normalized. This combined view demonstrates how each lncRNA's expression is influenced over time in the context of its spatial identity, providing deeper insights into the coordinated regulation of lncRNAs during regeneration.

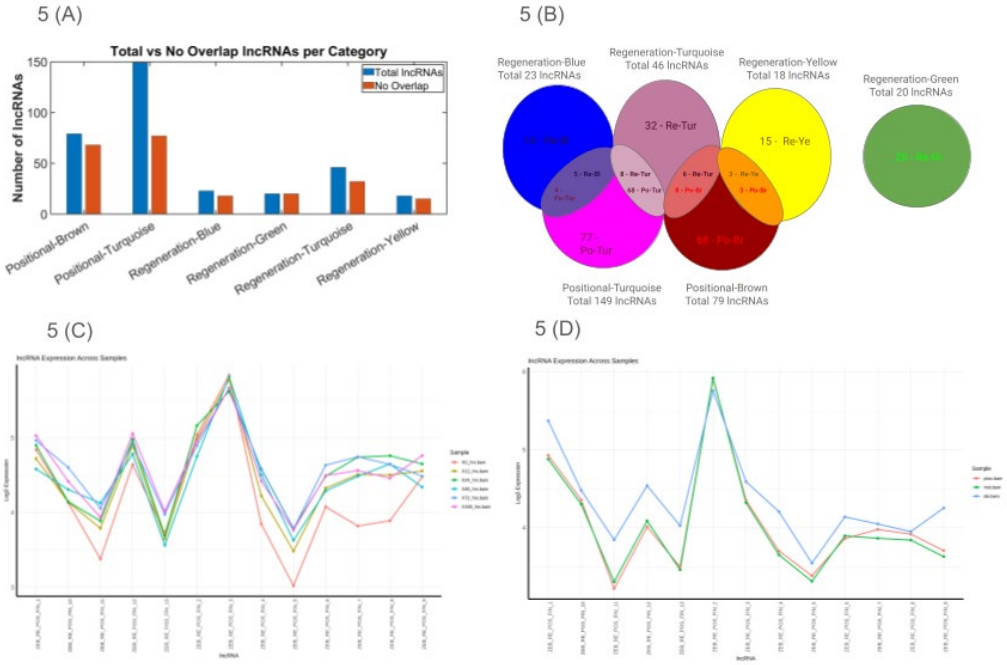

Figure 5. (A) number of total lncRNAs with non-overlapping lncRNAs, (B) how positional memory module lncRNAs overlapped with fin regeneration lncRNAs. For example, six Re-Tur are overlapped with eight Po-Br lncRNAs. (C), Expression varies in different positional points of each 13 lncRNAs, (D) Expression varies in different time points of each 13 lncRNAs.

2.4. WGCNA and Pathway Analysis with Overlapping Regions

After merging StringTie CSV files from both the regeneration and positional memory RNA-seq datasets, we created a count matrix, which was then normalized based on groups. The pipeline is provided in Figure 6. WGCNA analysis was performed on this normalized matrix, generating a dendrogram with 89 colour modules in Supplementary Document 6. We also performed PCA plotting and generated a heatmap to analyze sample-to-sample variations. Figure 7 presents a comprehensive expression analysis, including: A) a PCA plot of normalized RNA expression, B) a

 doi:10.20944/preprints202604.1402.v1

heatmap of sample-wise expression correlation, and C) a cluster-level heatmap showing expression correlations among regions containing the 13 overlapping lncRNAs.

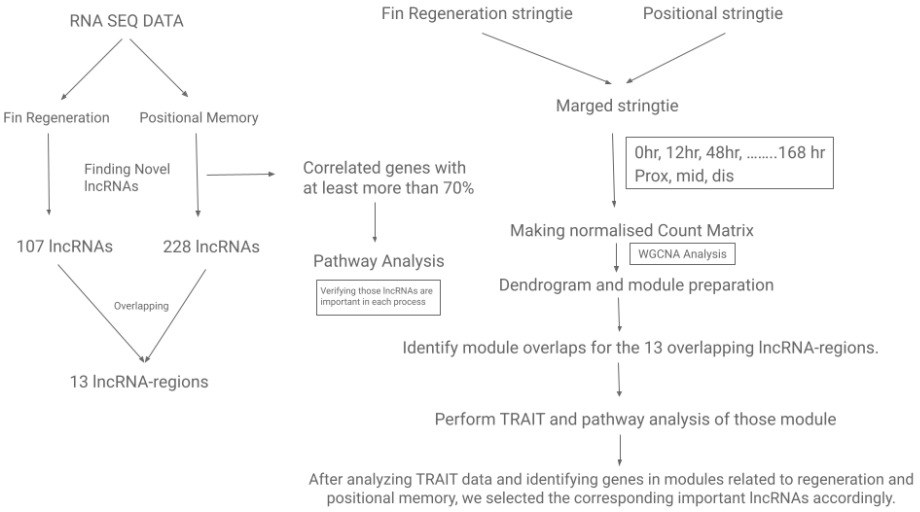

Figure 6. Schematic of the lncRNA verification pipeline.

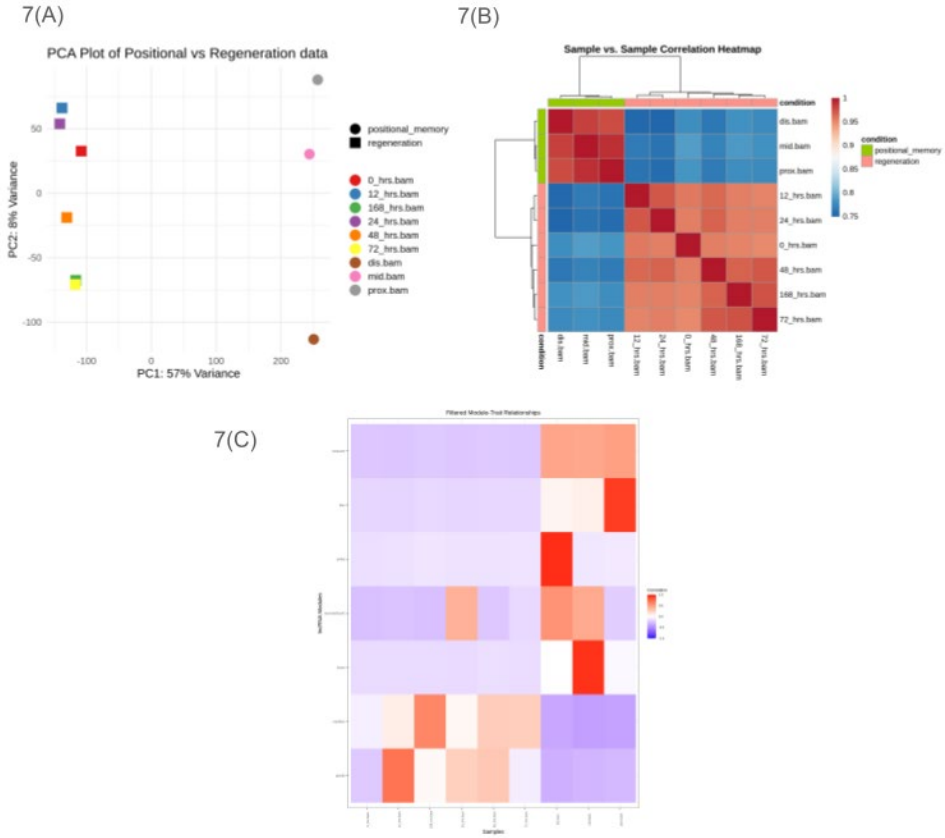

Figure 7. A) PCA plot of normalized RNA expression. B) Heatmap of RNA expression correlation between all samples. C) Heatmap showing the correlation of expression profiles among RNA clusters where all my overlapping 13 lncRNA-regions are present.

Next, we identified lncRNAs that fully overlap with the 13 previously detected overlapping lncRNA regions. Since merging the StringTie files modified the lncRNA names, we reassigned these

 doi:10.20944/preprints202604.1402.v1

regions to their corresponding modules. Our analysis confirmed that these regions are present in the turquoise, blue, yellow, lavenderblush2, brown, royal blue, and grey60 modules.

Finally, TRAIT analysis identified the brown, lavender blush 2, royal blue, and grey 60 modules as showing strong trends. Pathway enrichment analysis of these modules revealed multiple regeneration-related pathways; enrichment maps are shown in Supplementary Document 7. These pathways highlight the interplay between chromatin remodelling, epigenetic regulation, and DNA repair mechanisms that maintain genome stability during tissue regeneration.[59,60]. The dynamic regulation of chromatin accessibility, influenced by nucleosome positioning and epigenetic modifications, is key to facilitating efficient DNA recombination and repair [61]. Additionally, specific lipid signalling pathways and metabolic shifts have been shown to modulate regeneration in various tissues, including the liver and the nervous system [62]. The epidermal growth factor receptor (EGFR) and ErbB signalling pathways are also critical in tissue regeneration, regulating cellular processes such as proliferation, differentiation, and survival [62]. These pathways are particularly important in maintaining tissue integrity and promoting repair processes in organs like the intestine and liver [63]. Understanding the complex interactions between these pathways and processes is crucial for developing targeted therapeutic strategies to enhance tissue repair and regeneration in clinical settings.

In the lavenderblush2 module, the most crucial gene is DNase1. DNase1 plays a role in apoptosis and tissue remodelling, facilitating the removal of damaged cells and shaping new tissue growth [64,65]. TTLL9 is involved in microtubule modifications, particularly tubulin polyglutamylation, which is essential for cellular reorganization during regenerative processes [66,67]. FAM50A has been implicated in transcriptional regulation, potentially influencing the expression of genes necessary for regeneration, including its role in the spliceosome complex and modulation of cell proliferation and apoptosis. PLEKHD1 is thought to play a role in cellular signalling pathways involved in tissue repair and regeneration, potentially interacting with or influencing pathways similar to the well-studied Wnt/β-catenin and Notch signalling cascades [68,69]. The specific roles of CR855375.1, BX324179.1, CR388363.1, and CR847944.1 [70] in regeneration are currently undocumented. Their presence in the lavenderblush2 module, a co-expressed gene network potentially active during regeneration, suggests possible involvement in regenerative processes [71]. These lncRNA modules may be involved in crucial biological processes, such as cell proliferation, apoptosis, angiogenesis, and extracellular matrix remodelling, which are important for regeneration [72]. This presents an opportunity for targeted studies to elucidate their functions in tissue repair and regeneration [73].

In the royal blue module, the regenerative process involves a complex interplay of various genes, each contributing to specific aspects of tissue repair and renewal. Key players include id1, crucial for cell cycle regulation and stem cell maintenance [74], and hmgb1b, a DAMP protein facilitating wound healing [75]. Manf supports cell survival and tissue repair, while mafba contributes to development and regeneration [75]. Annexins (anxa1c and anxa5b) regulate inflammation and apoptosis, essential for wound healing [76]. Other significant genes include tk2 and exo5 for DNA repair, pde6gb for signalling, rnf169 for DNA damage repair, laptm4b for cell proliferation, cyp46a1.3 for lipid metabolism, irx6a for tissue development, stat2 for immune signalling, and cul2 for protein degradation and cell cycle regulation [77]. This diverse array of genes highlights the multifaceted nature of regeneration, encompassing processes from cellular repair to tissue-wide renewal. CR381540.3 and BX322787.1 are potentially crucial for zebrafish regeneration, influencing cell proliferation and inflammatory responses [78]. These modules of lncRNAs may regulate gene networks essential for wound healing and blastema formation, key processes in regeneration [11]. Further research is needed to elucidate their specific roles in regenerative signalling and cellular reprogramming, which could have implications for understanding tissue repair mechanisms [79].

For the grey60 module, the regenerative process involves a complex interplay of genes regulating various cellular mechanisms. Adam10a, casp6b.1, and srgn are crucial for tissue remodelling and repair, with roles in processes such as apoptosis, inflammation, and extracellular matrix remodelling [80]. Arid2 influences gene expression essential for regeneration, particularly in

 doi:10.20944/preprints202604.1402.v1

stem cell differentiation and osteoblast commitment [81]. Zbed4, rps9, and rab5b likely contribute to cell proliferation, protein synthesis, and cellular reprogramming, respectively, based on their known functions in related cellular processes [82]. Ube2l3b, as part of the ubiquitin-proteasome system, regulates protein degradation in regenerative signalling pathways, while tmem161a facilitates cell communication during regeneration through its role in signal transduction [83]. This module contains several lncRNAs previously known for their importance in regeneration, including H19, Linc-MD1, LncMyoD, Malat1, and SRA, which are primarily involved in muscle differentiation, tissue repair, and stem cell regulation [5]. The specific roles of BX548015.2, CU019562.3, CT027980.1, CT573366.1, BX088688.2, BX936391.1, CU681836.1, AL954138.2, and CR792438.1 [70] in regeneration are currently undocumented. Their presence in the grey_60 module, a co-expressed gene network potentially active during regeneration, suggests possible involvement in regenerative processes [84]. Additionally, this module includes lncRNAs that could play a significant role in regeneration, which require further investigation to determine their precise functions in wound healing, blastema formation, and cellular reprogramming [11].

The brown module contains several genes associated with regeneration, with some key lncRNAs playing crucial roles. Hypoxia-inducible factor 1-alpha (HIF-1α) regulates angiogenesis and osteogenesis by elevating VEGF levels in osteoblasts. Transforming growth factor-beta 1 (TGF-β1) signalling, activated under hypoxic conditions via HIF-1α, promotes collagen deposition, crucial for tissue repair. Additionally, HIF-1α is essential for bone regeneration, influencing various pathways in bone tissue engineering [85]. Additionally, CR381540.2 has been linked to cellular differentiation processes, which are vital for tissue regeneration, while CR788322.2 regulates gene expression during stress responses, potentially influencing regenerative outcomes. These lncRNA modules offer significant opportunities to understand molecular mechanisms of regeneration and warrant further investigation.

After WGCNA analysis and pathway enrichment, we identified four key lncRNA regions among the 13 overlapping lncRNA regions that play a major role: ZEB_RE_POS_FIN_2, ZEB_RE_POS_FIN_4, ZEB_RE_POS_FIN_5, and ZEB_RE_POS_FIN_11. These regions are distributed across multiple modules: ZEB_RE_POS_FIN_11 in grey60 and turquoise; ZEB_RE_POS_FIN_2 in brown, blue, and turquoise; ZEB_RE_POS_FIN_4 in lavenderblush2; and ZEB_RE_POS_FIN_5 in royal blue and turquoise. The list of all regions and their corresponding modules is provided in Supplementary Document 8.

Figure 5 (C) illustrates the expression variation of each lncRNA across different regeneration time points, highlighting temporal changes in transcriptional activity during the regenerative process. Figure 5 (D) shows the positional expression differences of the same lncRNAs across the proximal, median, and distal regions of the regenerating fin, emphasizing their region-specific regulation.

2.5. Validation of Selected lncRNAs

To validate our in silico findings, we selected the eight most effective lncRNA regions, ZEB_RE_POS_FIN_1, ZEB_RE_POS_FIN_2, ZEB_RE_POS_FIN_4, ZEB_RE_POS_FIN_5, ZEB_RE_POS_FIN_9, ZEB_RE_POS_FIN_11, ZEB_RE_POS_FIN_12, and ZEB_RE_POS_FIN_13, that displayed strong and stage-specific expression in the RNA-seq dataset. The qRT-PCR results confirmed that all eight regions exhibited clear, consistent expression at the specific regeneration time points predicted to be active. This alignment between experimental and computational data strengthens the biological relevance of these long non-coding RNA (lncRNA) regions. The validated expression patterns are presented in Figure 8, further supporting their potential role in fin regeneration. The results confirmed the stage-specific and dynamic regulation of these lncRNAs (Figures 5 and 8).

 doi:10.20944/preprints202604.1402.v1

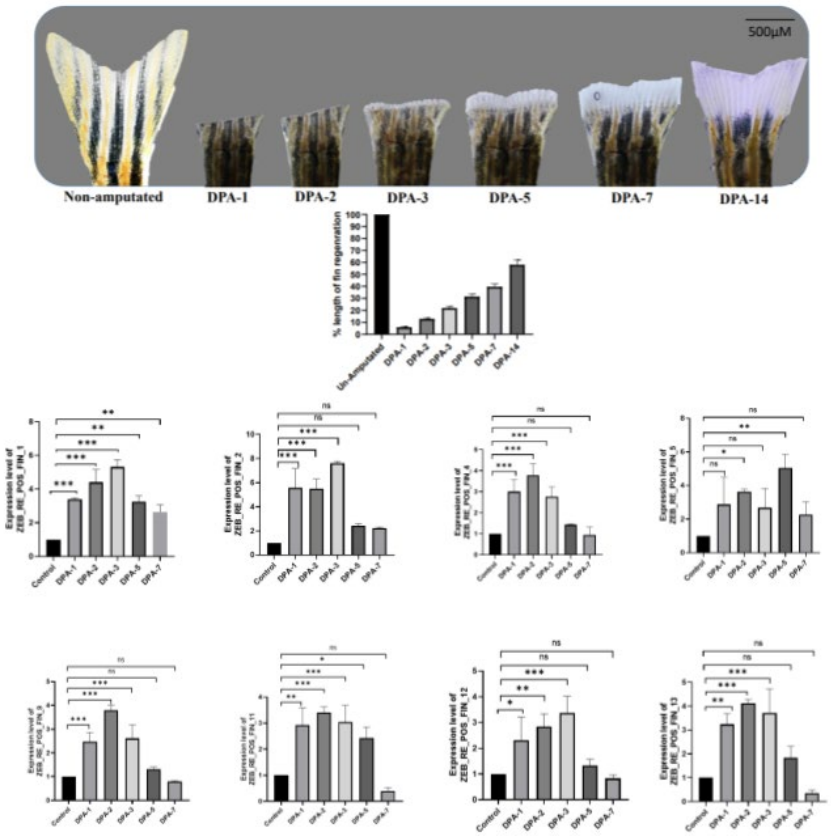

Figure 8. Expression of lncRNA-region in Zebrafish Caudal Fin Regeneration in Proximal Position.

Early induction (1–2 dpa): *ZEB_RE_POS_FIN_1, _2, _4, _9, and _11* were strongly upregulated as early as 1 dpa, peaking between 2 and 3 dpa. For example, *ZEB_RE_POS_FIN_1* showed ~5-fold induction at 2 dpa, while *ZEB_RE_POS_FIN_2* and *ZEB_RE_POS_FIN_9* showed ~7- to 8-fold upregulation compared to the control. These profiles suggest a role in wound healing, blastema formation, and early proliferative events.

Intermediate/later activity: *ZEB_RE_POS_FIN_5* and *ZEB_RE_POS_FIN_12* showed modest but significant induction at 2-3 dpa (~2–3 fold), indicating possible roles in the transition from proliferation to differentiation. *ZEB_RE_POS_FIN_13* peaked at 3 dpa (~5-fold), declining thereafter, consistent with functions in mid-regeneration events.

Decline at remodelling stage (7 dpa): Most lncRNAs (ex, *ZEB_RE_POS_FIN_1, _2, _4, _9, _11, _13*) showed reduced expression by 7 dpa, suggesting their functions are temporally restricted to early and intermediate regeneration phases.

Overall, the temporal expression profiles demonstrated a strong concordance between computational predictions and experimental validation (Figure 5A). Their expression dynamics highlight the importance of further investigation into these lncRNA regions, which were identified through PhastCons conservation analysis and also exhibit positional memory characteristics. Together, these findings suggest that these lncRNAs may play critical roles in regenerative processes and could potentially serve as conserved regulators of regeneration in other species.

To support the positional relevance of our identified lncRNAs across multiple species, we performed qPCR on days 1, 3, and 7 in both the proximal, median, and distal regions of the regenerating tissue (Figures 8, 9, and 10). The results revealed distinct expression patterns at each position at the time point, indicating early induction, Intermediate activity, and remodelling stages, suggesting that these lncRNAs are not only position- and time-specific but may also play important roles in evolutionarily conserved regenerative processes.

 doi:10.20944/preprints202604.1402.v1

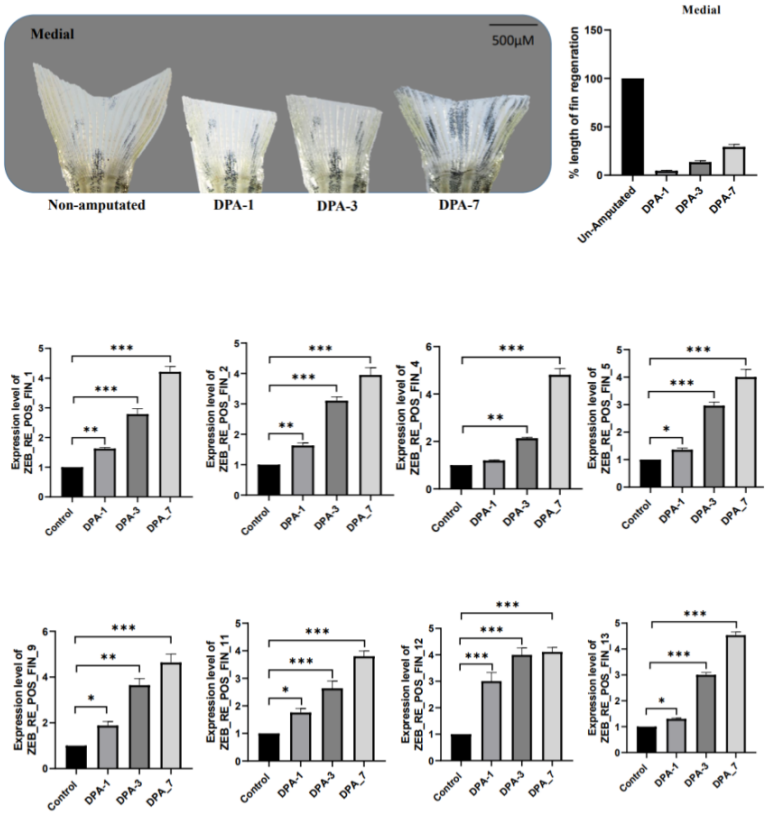

Figure 9. Expression of lncRNA-region in Zebrafish Caudal Fin Regeneration in Medial Position.

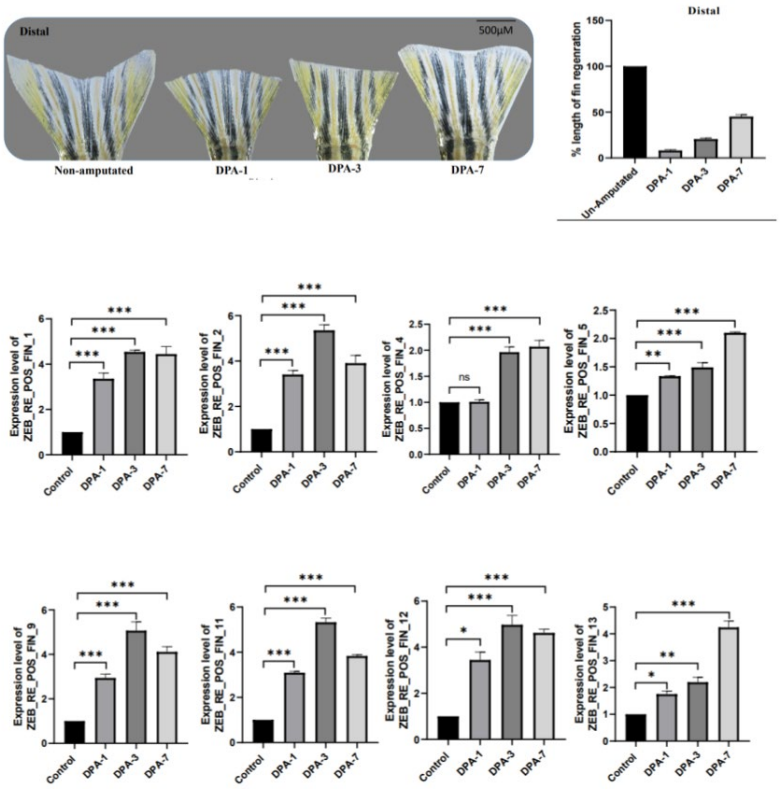

Figure 10. Expression of lncRNA-region in Zebrafish Caudal Fin Regeneration in Distal Position.

 doi:10.20944/preprints202604.1402.v1

ZEB_RE_POS_FIN_1 exhibited a marked downregulation by day 7 in the proximal fin region, whereas in the median and distal regions, its expression peaked around day 3 of regeneration, suggesting a region-specific temporal expression pattern. ZEB_RE_POS_FIN_2 displayed an upward trend in expression in the median fin region, while in the proximal and distal regions, its expression declined significantly after day 3. Notably, expression in the distal region remained consistently low throughout the regeneration timeline. ZEB_RE_POS_FIN_4 showed markedly low expression in the proximal region by day 7, while the median region exhibited a consistent upward trend throughout regeneration. Although the distal region also followed an increasing trend, its expression remained relatively low from day 3 onward. ZEB_RE_POS_FIN_5 exhibited a downward trend in the proximal region, while both the median and distal regions showed an upward trend in expression. However, the increase in the median region was comparatively less pronounced. ZEB_RE_POS_FIN_9 shows a peak at Day 3 in the proximal and distal regions, followed by a decline by Day 7, while in the median region, expression steadily increases from Day 1 to Day 7, reaching its highest level at DPA-7. ZEB_RE_POS_FIN_11 exhibited a sharp upregulation by Day 3 in both the median and distal regions, followed by a sustained high or slightly decreased expression by Day 7. In contrast, the proximal region showed an early increase at Day 1 and Day 3, but a sharp drop in expression by Day 7, suggesting a transient activation pattern unique to this region. ZEB_RE_POS_FIN_12 showed a transient expression peak at Day 3 in the proximal region, followed by a clear downregulation by Day 7. In contrast, both the median and distal regions demonstrated a strong and sustained upregulation from Day 1 through Day 7, with no significant drop in expression. ZEB_RE_POS_FIN_13 also exhibited a distinct expression pattern in the proximal region compared to the median and distal regions, indicating region-specific regulation during regeneration.

In summary, the qPCR data not only validate the 3-day expression patterns shown in Figure 7(D), but also reveal clear temporal and positional dynamics of lncRNA expression across the fin during regeneration. Distinct trends were observed across the proximal, median, and distal regions. In the proximal region, lncRNAs displayed a transient expression profile, peaking around Day 2 or 3 and then declining sharply by Day 7, indicating early but short-lived involvement. The median region exhibited a gradual and sustained increase from Day 1 to Day 7, suggesting continuous regulatory activity throughout regeneration. In contrast, the distal region showed robust and consistently high expression levels from early to late stages, reflecting persistent activation. Together, these findings emphasize the spatially and temporally distinct roles of lncRNAs in coordinating the regenerative response across different fin regions.

3. Discussion

Our study identifies a set of lncRNA regions that are spatiotemporally regulated during zebrafish caudal fin regeneration, integrating both regeneration time-course and positional memory datasets. By overlapping these datasets, we identified 13 lncRNA genomic regions that are consistently present during key regenerative stages, span the proximodistal axis over time, and are also conserved across multiple models. Experimental validation via qRT-PCR confirmed their stage-specific expression, particularly during blastema formation and regenerative outgrowth, aligning with our computational predictions. These results highlight that lncRNAs serve as dynamic molecular regulators, linking positional identity with regenerative progression.

To identify these novel long non-coding RNAs (lncRNAs), we developed a comprehensive bioinformatics pipeline. RNA-seq reads from both datasets were quality-checked and aligned using HISAT2, and transcripts were assembled with StringTie to create sample-specific transcriptomes. FEELnc was used to filter and classify lncRNAs based on coding potential and genomic context, while WGCNA co-expression analysis linked lncRNAs to relevant gene modules associated with regeneration and positional memory. PhastCons conservation scoring was then applied to prioritize evolutionarily constrained regions. We also recheck the effectiveness of lncrnas-region via doing a full WGCNA analysis with all other RNAs, and final candidates were validated against RNA-seq

 doi:10.20944/preprints202604.1402.v1

expression profiles and qRT-PCR results, ensuring that only robust, biologically relevant lncRNAs were selected.

The temporal expression profiles of the validated lncRNAs further reinforce their potential role in coordinating positional memory with regenerative progression. For instance, lncRNAs peaking at early stages (1-2 dpa) overlapped with transcripts enriched in proximal and middle fin compartments, consistent with their association with blastema initiation and proliferative cues. Conversely, those induced at intermediate stages (3-5 dpa) aligned with positional signatures from distal compartments, suggesting involvement in differentiation and patterning processes. This convergence across datasets underscores that lncRNAs are not only time-specific regulators of regeneration but also spatially tuned, providing a molecular link between positional identity and regenerative outcome.

Importantly, the conservation analysis suggests that several of these lncRNA regions are evolutionarily conserved, raising the exciting possibility of identifying universal lncRNAs that may govern regeneration across species. Exploring these regions in mammals or other vertebrates could uncover latent regenerative mechanisms, potentially enabling the design of lncRNA-based therapeutic strategies. From a future perspective, functional characterization of these candidates through knockdown, overexpression, or CRISPR-based perturbation approaches will be critical to establish their roles in regeneration. Such studies could bridge descriptive profiling with mechanistic insights and may ultimately guide translational efforts in regenerative medicine.

Our findings thus provide a foundation for cross-species studies, moving closer to defining core non-coding RNA regulators that could one day enhance tissue repair and regeneration in species with limited regenerative capacity.

4. Materials and Methods

The methodology for this study comprises five primary steps, as depicted in Figure 11A under the heading “Basic Approach Methodology.” Furthermore, Figure 11B also provides a comprehensive schematic of the lncRNA discovery pipeline, detailing each stage involved in the identification and characterization of long non-coding RNAs.

 doi:10.20944/preprints202604.1402.v1

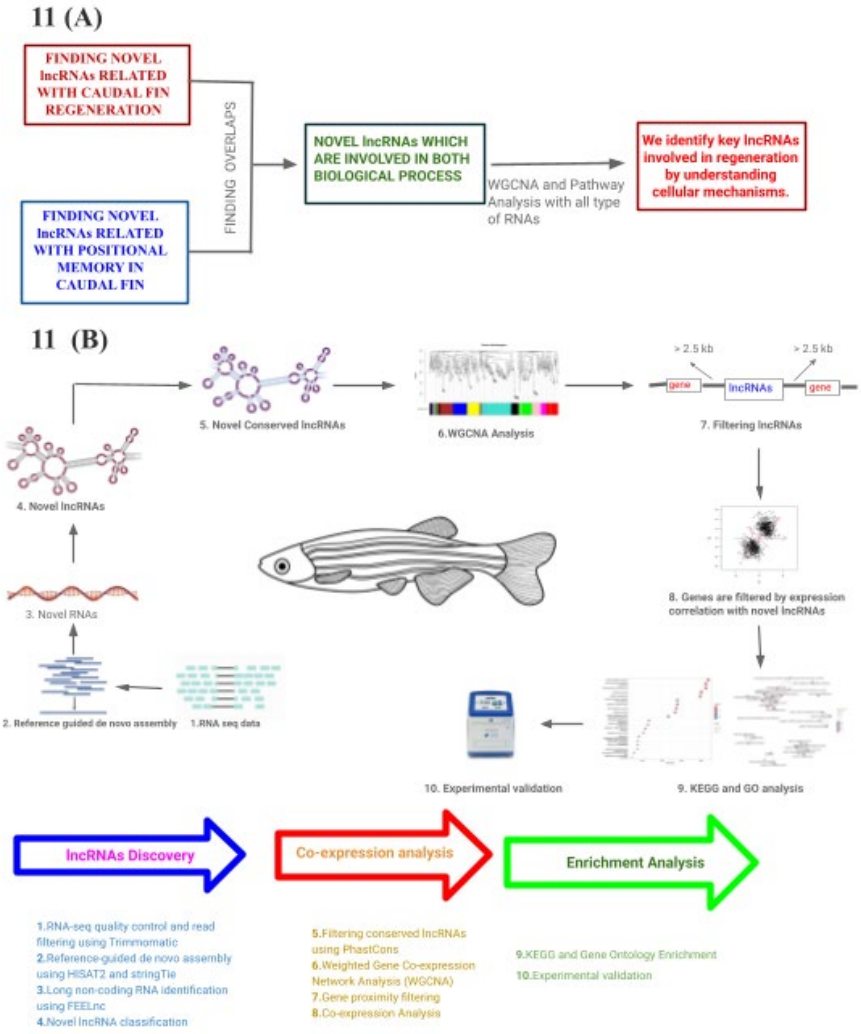

Figure 11. (A) Our Basic Approach Methodology, (B)Schematic of the lncRNA discovery pipeline.

4.1. Novel LNCRNA Identification Methodology

4.1.1. Data Acquisition and Sample Description

FOR CAUDAL FIN REGENERATION:

RNA sequencing data were obtained from the NCBI database under the Bio Project accession number PRJNA248169, as part of a study conducted by Banu, S. et al., 2022, [86]. The data were analyzed to assess lncRNA expression at various time points: 0 hours post-amputation (hpa), 12 hpa, 1-day post-amputation (dpa), 2 dpa, 3 dpa, and 7 dpa. These time points capture the sequential phases of regeneration, beginning with inflammation and wound healing (0–12 hpa), followed by blastema formation and proliferative expansion (1–3 dpa), and culminating in tissue patterning and remodelling (7 dpa). Morphological landmarks were also noted, with bony ray (lepidotrichia) formation evident between 2–3 dpa, and actinotrichia aligned along the proximal–distal axis by 7 dpa (Figure 12A) [86].

 doi:10.20944/preprints202604.1402.v1

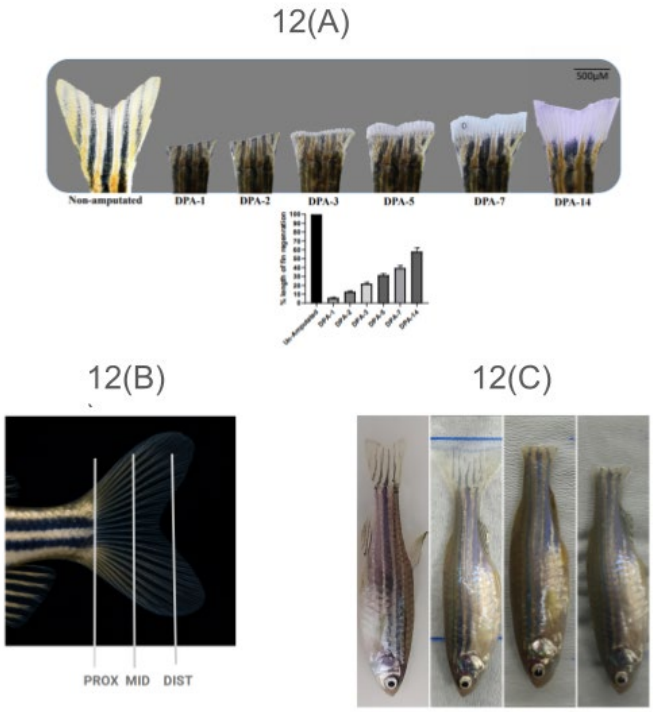

Figure 12. (A) Representative photos illustrating gradual caudal fin regrowth in adult zebrafish after proximal amputation. Caudal fins were severed at the proximal level (0 DPA), and regeneration was observed at consecutive time points: 1, 2, 3, 5, 7, and 14 days post-amputation (DPA). The un-amputated fin (far left) illustrates the baseline full-length fin. Images indicate the steady and ordered re-growth of fin tissue over time, with considerable morphological repair visible by DPA-14. All photos are scaled to the same magnification; scale bar = 500 μm. (B) Schematic representation of the zebrafish caudal fin illustrating the three defined regions along the proximodistal axis: proximal (PROX), middle (MID), and distal (DIST). (C) Representative dorsal view images of adult zebrafish showing intact caudal fin (first panel), fin amputated at the distal region (second panel), fin amputated at the middle region (third panel), and fin amputated at the proximal region (fourth panel).

FOR POSITIONAL MEMORY:

RNA sequencing data utilized in this study were obtained from the Gene Expression Omnibus (GEO) database (accession no. GSE92760) and were originally generated as part of the study, Transcriptomic, Proteomic, and Metabolomic Landscape of Positional Memory in the Caudal Fin of Zebrafish by Rabinowitz et al. [87,88]. The dataset consists of RNA-seq profiles from five biological replicates for each of three distinct regions along the proximodistal axis of the zebrafish caudal fin: proximal, middle, and distal (totalling 15 samples). Each biological replicate represents pooled fin tissue collected from two male and two female zebrafish [87,88] (Figure 12B).

Together, these two datasets enable parallel investigation of temporal lncRNA dynamics during regeneration and spatial lncRNA signatures underlying positional memory, offering a comprehensive view of molecular mechanisms driving zebrafish caudal fin regrowth.

4.1.2. Transcriptome Assembly and Mapping

FASTQ files corresponding to each sample were retrieved from the NCBI Sequence Read Archive (SRA) using their respective Bio Project accession numbers. The raw sequencing reads underwent quality control and preprocessing using Trimmomatic (v0.38) [89], with adapter sequences removed and low-quality bases trimmed using default parameters to ensure high-quality downstream analysis. The resulting cleaned reads were then aligned to the Danio rerio reference genome (GRCz11) using HISAT2 (v2.2.1)[90]. During alignment, the --no-templatelen-adjustment parameter was used to disable template length correction, which is more suitable for RNA-seq data

 doi:10.20944/preprints202604.1402.v1

and helps maintain transcript-level alignment accuracy. StringTie (v2.2.1) [91] was used for reference-guided transcript assembly with reverse-stranded libraries, using HISAT2 outputs and merging all sample transcriptomes.

4.1.3. Identification and Classification of lncRNAs

For annotation and classification, we applied FEELnc (v0.2.1) [92], a machine learning–based framework specifically designed to distinguish lncRNAs from protein-coding transcripts. Unlike alignment-dependent methods, FEELnc relies on a Random Forest classifier trained on multi-k-mer frequency patterns and relaxed ORF features, allowing it to capture subtle differences between coding and noncoding sequences. To improve the reliability of our dataset, we used the filtering modules provided within the pipeline: FEELnc_filter.pl to exclude likely artifacts such as mono-exonic transcripts, and FEELnc_codpot.pl to evaluate and remove sequences with coding potential [92]. The remaining transcripts were then organized by genomic context and proximity to annotated genes, yielding a curated set of high confidence lncRNAs for downstream analysis.

4.1.4. Conservation Analysis

To evaluate whether the lncRNAs we identified showed evidence of evolutionary preservation, we analyzed their sequences with PhastCons (v1.6) [93], which applies a phylogenetic hidden Markov model to estimate conservation scores across species. Because multiple sequence alignment (MSA) data were not directly available for the updated zebrafish genome build, we first converted transcript coordinates to the appropriate reference version using BedFile Liftover, ensuring compatibility with the conservation framework. This allowed us to reliably assess which lncRNAs carry signatures of cross-species conservation, a feature often associated with functional relevance.

4.1.5. Weighted Gene Co-Expression Network Analysis (WGCNA)

To explore higher-order relationships among transcripts, we applied Weighted Gene Co-expression Network Analysis (WGCNA) [94] using the R package (v1.72-5). Prior to network construction, expression values were TPM-normalised to reduce technical bias and make samples comparable. In building the network, we selected a soft-thresholding power of 30, as this value best satisfied the scale-free topology criterion, ensuring that the resulting network captured biologically realistic patterns of connectivity. We focused on a signed network, which gives greater weight to positive correlations, and organized the data with parameters tuned for sensitivity: a deep split level of 2, a minimum module size of 30 transcripts, and a block size capped at 4000 genes. Modules were merged when their similarity exceeded a cut height of 0.25, preventing fragmentation of closely related clusters. Through this process, we obtained groups of co-expressed genes and lncRNAs that highlight coordinated biological activity and point toward regulatory programs relevant to the processes under study.

4.1.6. Gene Proximity Analysis

After identifying key modules using WGCNA, we refined the candidate lncRNA set by considering their genomic neighbourhoods. Using coordinate information extracted from reference GTF annotations and the StringTie assemblies, we checked whether each lncRNA lay within 2.5 kb of a known coding gene. Those falling inside this window were removed from further consideration, as they might represent transcriptional noise or extensions of nearby transcripts rather than independent loci. To further strengthen the functional relevance of the modules, we re-examined co-expression patterns between lncRNAs and protein-coding genes. Our guiding principle was that transcripts that rise and fall together are more likely to participate in related processes. For this reason, we used Pearson's correlation analysis and retained only strong relationships (correlation coefficients≥ 0.75). Within these networks, particular emphasis was placed on lncRNAs that

 doi:10.20944/preprints202604.1402.v1

repeatedly occupied central or hub-like positions, as these were more likely to play important biological roles.

4.1.7. Pathway Enrichment Analysis

To understand the functional context of the novel lncRNAs uncovered in our dataset, we examined the genes that were consistently co-expressed with them and asked what kinds of biological activities these associations might imply. For this purpose, we relied on the ClusterProfiler [95] package in R, which allowed us to link expression clusters to well-annotated functional categories. Instead of simply listing the genes, we traced their connections to established Gene Ontology processes and KEGG signalling pathways, using all expressed transcripts as a reference background to avoid bias. Only associations that passed a conservative statistical cutoff ($p < 0.05$) were considered meaningful. By taking this approach, we were able to highlight functional patterns suggesting roles for lncRNAs in developmental regulation, tissue physiology, and regenerative biology, while also prioritizing specific candidates for further experimental work.

4.2. Finding Overlaps

We aim to identify the overlap among novel lncRNAs that play crucial roles in different biological processes, particularly those involved in fin regeneration and positional memory. By analyzing these lncRNAs, we aim to identify those that are consistently essential across multiple regenerative stages and in spatial identity regulation. This approach allows us to uncover key regulatory lncRNAs that not only drive regeneration but also maintain positional cues within the tissue. Identifying such lncRNAs could provide deeper insights into the molecular mechanisms underlying regeneration and spatial patterning, potentially leading to broader applications in regenerative medicine.

4.3. WGCNA and Pathway Analysis

We performed WGCNA to analyze all RNAs from the RNA-seq dataset on regeneration and positional memory, obtained from the NCBI database (PRJNA248169 and GEO accession no. GSE92760), and identified overlapping lncRNAs that are crucial for both biological processes. WGCNA (v1.72-5) was used to detect co-expressed genes and lncRNA clusters, with normalized data and a soft-thresholding power of 30, ensuring a scale-free network. A signed network was constructed with a deep split level of 2, a minimum module size of 30 genes, and a maximum block size of 4000 genes, merging related modules at a cut height of 0.25.

Pathway enrichment analysis using ClusterProfiler linked novel lncRNA clusters to key biological functions and pathways. Gene Ontology (GO) and KEGG enrichment were performed with a P-value threshold of <0.05, using all expressed genes as the background. This analysis provided valuable insights into the functional roles of lncRNAs in zebrafish development, regeneration, and positional memory.

4.4. Zebrafish Maintenance and Induction of Stab Wound Injury

Adult zebrafish (3 months old, 25–30 mm length) were maintained under standard laboratory conditions. For fin amputation, fish were anesthetized in freshly prepared 0.02% Tricaine solution (diluted in system water), with complete anaesthesia confirmed when the animals became immobile within 40–60 seconds [96,97]. At 0 days post-amputation (DPA), the caudal fin was amputated at the proximal position, i.e., at the level where the fin rays emerge from the peduncle, using a sterile surgical blade (No. 11 scalpel). All amputations were performed uniformly across experimental animals. Following surgery, fish were transferred to fresh tank water under normal housing conditions to facilitate regeneration. Regenerating fins were imaged at 1, 2, 3, 5, and 7 dpa using a stereo microscope (SMZ1270) equipped with a digital camera. Fin regeneration was quantified using

 doi:10.20944/preprints202604.1402.v1

ImageJ software (NIH, USA) by calculating the total regenerated fin area at each time point relative to the pre-amputation fin area (set at 100%).

4.5. RNA Isolation, cDNA Synthesis, and qRT-PCR

The experiments were conducted using AB strain zebrafish (3–4 months old). Total RNA was extracted from tissue samples using Trizol reagent (Invitrogen, 15596026), followed by phase separation with chloroform (Merck, 1.94506.0521) and precipitation with isopropanol (Sigma, I9516). RNA quantity and purity were assessed using a Nanodrop™ One/OneC Microvolume UV-Vis Spectrophotometer (Thermo Scientific, ND-ONE-W). First-strand cDNA was synthesized using the TAKARA cDNA synthesis kit (6110A), and qRT-PCR reactions were set up with iTaq Universal SYBR Green Super mix (Bio-Rad, 1725121). The reactions were performed in hard-shell PCR plates (Bio-Rad, HSP9601) sealed with Bio-Rad plate sealers (MSB1000) on a CFX96 Touch Deep Real-Time PCR Detection System (Bio-Rad, 1854096). Nuclease-free water (Qiagen, 129115) was used for all reactions, and gene-specific real-time primers (Eurofins) were employed for amplification. Tissue homogenization was performed using a Jaisbo MT-13K homogenizer, and sample dissection and phenotypic observation were carried out using a Nikon Trinocular Stereo Zoom Microscope (SMZ1270).

To assess the temporal expression profile of selected long non-coding RNAs (lncRNAs) during caudal fin regeneration, total RNA was isolated from the proximal region of regenerating caudal fins at multiple time points: 1, 2, 3, 5, and 7-day post-amputation (DPA) and for distal and median region we done for time point: 1, 3, and 7 DPA. Fin samples were collected in RNase-free conditions, and RNA extraction was performed using the Trizol (Invitrogen, catalogue number: 15596026) according to the manufacturer's protocol. The purity and concentration of RNA were measured using a Nanodrop™ spectrophotometer. For cDNA synthesis, 1 μg of total RNA from each sample was reverse transcribed using the TAKARA cDNA synthesis kit (catalogue number: 6110A) according to the recommended protocol. Quantitative real-time PCR (qPCR) was performed using iTaq Universal SYBR Green Super mix (Bio-Rad, catalogue number 1725121). Each reaction was performed in triplicate. Expression levels of eight selected lncRNAs were quantified, and relative gene expression was calculated using the 2^−ΔΔCt method, with RPL13a as the Internal control.

5. Conclusions

Our study shows that conserved lncRNAs may play important roles in zebrafish fin regeneration and could become future targets for regenerative medicine.

1. We analyzed RNA-seq data from six regeneration time points and three positional regions, identifying 107 long non-coding RNAs (lncRNAs) linked to regeneration timing and 229 associated with positional memory.

2. Identification of 13 regeneration-active lncRNAs with strong positional specificity, suggesting a core set of molecular regulators that may be conserved across species.

3. Experimental validation showing that these lncRNAs directly influence spatial patterns of tissue regrowth, revealing new pathways through which non-coding RNAs modulate protein activity and regenerative decisions.

Supplementary Materials: The following supporting information is given with the article. Supplementary Document 1.: Bar chart shows the distribution of genomic regions based on their PhastCons conservation scores, with most regions falling into high-score bins, indicating strong evolutionary conservation across species. Supplementary Document 2.: lnc-RNAs which are important for fin regeneration. Supplementary Document 3.: lnc-RNAs which are important for fin positional memory**.** Supplementary Document 4.: The list of overlapping lncRNAs**.** Supplementary Document 5.: A more detailed, integrative analysis is here where BAM files from various time points were merged with those from the positional memory dataset and normalized. Supplementary Document 6.: WGCNA analysis was performed on this normalized matrix, generating a dendrogram with 89 colour modules**.** Supplementary Document 7.: pathway enrichment analysis, and the

 doi:10.20944/preprints202604.1402.v1

enrichment maps (EMap) of the selected module. Supplementary Document 8.: The list of all regions and their corresponding modules.

Author Contributions: Soumyadeep Paul: Conceptualized and designed the study; curated and analyzed publicly available zebrafish regeneration datasets with a specific focus on positional memory; developed and automated the lncRNA discovery pipeline. Identified novel lncRNAs associated with both regeneration and positional memory, and established a comparative framework to relate positional memory signatures with time-resolved regeneration data to capture dynamic regulatory changes. Performed integrative analyses to identify lncRNAs with shared and distinct roles across spatial and temporal contexts; conducted position- and time-specific expression profiling; and identified key lncRNAs with consistent differential expression across datasets. Validated candidate lncRNAs through correlation with regeneration-associated genes and assessed their potential evolutionary conservation. Designed the qPCR validation strategy, including primer design and fin dissection protocol. Interpreted findings in light of existing literature and prepared the complete manuscript with integrated data, figures, and validation results. A Hariharan: Maintained and handled zebrafish lines; performed fin amputations following the experimental protocol; extracted RNA, synthesized cDNA, conducted RT-PCR experiments, and provided the resulting expression graphs for analysis. Dasari Abhilash and Surbhi Kohli: Provided overall guidance and critical input throughout the course of the study. Dr. Shilpi Minocha: Conceived and supervised the overall project; supported funding and execution of wet-lab procedures; assisted in analysis and interpretation of experimental results, and provided continuous guidance throughout all stages of the study, from concept to completion. Dr. Ishaan Gupta: Conceived and supervised the overall project; provided the original idea, supported funding in the dry lab experiment, and provided continuous guidance throughout all stages of the study, from concept to completion.

Funding: IG was supported by the funds from the Department of Biotechnology, Government of India, through Ramalingasami fellowship ST/HRD/35/02/200 and Intramural MFIRP grant by IIT Delhi MI02552G to Ishaan Gupta. Soumyadeep Paul was supported by the Indian Institute of Technology Delhi through a student fellowship. Surbhi Kohli was supported by the Indian Institute of Technology Delhi through a postdoctoral fellowship. This research was also supported by the Council of Scientific & Industrial Research, Ministry of Science and Technology, Government of India, through CSIR-JRF fellowship 09/086(1458)/2020-EMR-I to Dasari Abhilash. We are grateful for their support and funding, which enabled us to conduct this study. SM is supported by a Start-Up Research Grant from the Science and Engineering Board (SRG/2021/000341), a Ramalingaswami re-entry fellowship from the Department of Biotechnology (BT/RLF/Re-entry/70/2017), and IFCPAR/CEFIPRA (Indo-French Centre for Promotion of Advanced Research/Centre Franco-Indien pour la Promotion de la Recherche Avancée) grant no. 6503-J.

Data Availability Statement: The RNA sequencing data used for the positional memory analysis were obtained from the Gene Expression Omnibus (GEO) under the accession number GSE92760. The RNA-seq data used for the regeneration time-course analysis were retrieved from the NCBI Sequence Read Archive (SRA) under the BioProject accession number PRJNA248169. All processed and intermediate files generated during this study are available from the corresponding author upon reasonable request.

Acknowledgments: I would like to thank my supervisor and collaborators for their invaluable guidance and support throughout this study. I am also grateful to my lab colleagues for their assistance and constructive feedback, and to the funding agencies that made this research possible.

Conflicts of Interest: All authors declare that they have no competing interests.

References

1. Ferrer, J.; Dimitrova, N. Transcription regulation by long non-coding RNAs: mechanisms and disease relevance. *Nat. Rev. Mol. Cell Biol.* **2024**, *25*, 396–415, https://doi.org/10.1038/s41580-023-00694-9.
2. Llobat, L. Pluripotency and Growth Factors in Early Embryonic Development of Mammals: A Comparative Approach. *Veter- Sci.* **2021**, *8*, 78, https://doi.org/10.3390/vetsci8050078.

 doi:10.20944/preprints202604.1402.v1

3. Zhang, K.; Huang, K.; Luo, Y.; Li, S. Identification and functional analysis of long non-coding RNAs in mouse cleavage stage embryonic development based on single cell transcriptome data. *BMC Genom.* **2014**, *15*, 1–12, https://doi.org/10.1186/1471-2164-15-845.
4. e Silva, J.T.; Pessoa, J.; Nóbrega-Pereira, S.; de Jesus, B.B. The Impact of Long Noncoding RNAs in Tissue Regeneration and Senescence. *Cells* **2024**, *13*, 119, https://doi.org/10.3390/cells13020119.
5. Statello, L.; Guo, C.-J.; Chen, L.-L.; Huarte, M. Gene regulation by long non-coding RNAs and its biological functions. *Nat. Rev. Mol. Cell Biol.* **2021**, *22*, 96–118, doi:10.1038/s41580-020-00315-9; Correction in **2021**, *22*, 159, doi:10.1038/s41580-021-00330-4.
6. Duda, G.N.; Geissler, S.; Checa, S.; Tsitsilonis, S.; Petersen, A.; Schmidt-Bleek, K. The decisive early phase of bone regeneration. *Nat. Rev. Rheumatol.* **2023**, *19*, 78–95, https://doi.org/10.1038/s41584-022-00887-0.
7. Luo, S.; Lu, J.Y.; Liu, L.; Yin, Y.; Chen, C.; Han, X.; Wu, B.; Xu, R.; Liu, W.; Yan, P.; et al. Divergent lncRNAs Regulate Gene Expression and Lineage Differentiation in Pluripotent Cells. *Cell Stem Cell* **2016**, *18*, 637–652, https://doi.org/10.1016/j.stem.2016.01.024.
8. Zheng, L.; Liu, X.; Chen, P.; Xiao, W. Expression and role of lncRNAs in the regeneration of skeletal muscle following contusion injury. *Exp. Ther. Med.* **2019**, *18*, 2617–2627, https://doi.org/10.3892/etm.2019.7871.
9. Li, J.; Cai, H.; Chen, Y.; Pi, R.; Xiang, L.; Lu, Z.; Zhou, Y.; Wang, L. Long noncoding RNA LncBAR enhances BRG1 protein to promote cardiomyocyte cell cycle progression and cardiac repair. *npj Regen. Med.* **2025**, *10*, 52, https://doi.org/10.1038/s41536-025-00439-6.
10. King, B.L.; Rosenstein, M.C.; Smith, A.M.; Dykeman, C.A.; Smith, G.A.; Yin, V.P. RegenDbase: a comparative database of noncoding RNA regulation of tissue regeneration circuits across multiple taxa. *npj Regen. Med.* **2018**, *3*, 1–13, https://doi.org/10.1038/s41536-018-0049-0.
11. Mattick, J.S.; Amaral, P.P.; Carninci, P.; Carpenter, S.; Chang, H.Y.; Chen, L.-L.; Chen, R.; Dean, C.; Dinger, M.E.; Fitzgerald, K.A.; et al. Long non-coding RNAs: definitions, functions, challenges and recommendations. *Nat. Rev. Mol. Cell Biol.* **2023**, *24*, 430–447. https://doi.org/10.1038/s41580-022-00566-8
12. Pansera, L.; Mhalhel, K.; Cavallaro, M.; Aragona, M.; Laurà, R.; Levanti, M.; Guerrera, M.C.; Abbate, F.; Germanà, A.; Montalbano, G. Zebrafish as an Integrative Model for Central Nervous System Research: Current Advances and Translational Perspectives. *Life* **2025**, *15*, 1751, https://doi.org/10.3390/life15111751.
13. Mathew, M.M.; Prasad, K. Model systems for regeneration:*Arabidopsis*. *Development* **2021**, *148*, https://doi.org/10.1242/dev.195347.
14. Howe, K.; Clark, M.D.; Torroja, C.F.; Torrance, J.; Berthelot, C.; Muffato, M.; Collins, J.E.; Humphray, S.; McLaren, K.; Matthews, L.; et al. The zebrafish reference genome sequence and its relationship to the human genome. *Nature* **2013**, *496*, 498–503, doi:10.1038/nature12111
15. Kohli S, Abhilash D, Hemlata, Srivastava PP, Kumar V, Minocha S, et al. Discovery of Novel Long Non-Coding RNAs with potential role in zebrafish brain regeneration. bioRxiv. 2024. doi:10.1101/2024.06.03.597135
16. Goessling, W.; North, T.E. Repairing quite swimmingly: advances in regenerative medicine using zebrafish. *Development* **2014**, *141*, e1406–e1406, https://doi.org/10.1242/dev.114751.
17. Rosati, D.; Palmieri, M.; Brunelli, G.; Morrione, A.; Iannelli, F.; Frullanti, E.; Giordano, A. Differential gene expression analysis pipelines and bioinformatic tools for the identification of specific biomarkers: A review. *Comput. Struct. Biotechnol. J.* **2024**, *23*, 1154–1168, https://doi.org/10.1016/j.csbj.2024.02.018.
18. Ton, Q.V.; Iovine, M.K. Identification of an evx1-Dependent Joint-Formation Pathway during FIN Regeneration. *PLOS ONE* **2013**, *8*, e81240, https://doi.org/10.1371/journal.pone.0081240.
19. Macrae, T.A.; Fothergill-Robinson, J.; Ramalho-Santos, M. Regulation, functions and transmission of bivalent chromatin during mammalian development. *Nat. Rev. Mol. Cell Biol.* **2022**, *24*, 6–26, https://doi.org/10.1038/s41580-022-00518-2.
20. Khan, S.; Ahmad, K.; Liu, X.; Liang, Y. Unlocking the Potential of Retinoic Acid: A Comprehensive Review of Its Regulatory Role in Epimorphic Regeneration in Axolotl Limbs for Regenerative Medicine. *Regen. Eng. Transl. Med.* **2025**, 1–22, https://doi.org/10.1007/s40883-025-00407-y.
21. Bhatt R, Prasad R, Aswini S, Paul S, Gupta I. Automated Eight-Stage Classification of Drosophila melanogaster Using Transfer-Learning CNNs with Mobile Live-Inference Deployment. Bioinformatics. bioRxiv; 2025. Available: https://www.biorxiv.org/content/10.1101/2025.09.19.677285v1

 doi:10.20944/preprints202604.1402.v1

22. Wang, R.N.; Green, J.; Wang, Z.; Deng, Y.; Qiao, M.; Peabody, M.; Zhang, Q.; Ye, J.; Yan, Z.; Denduluri, S.; et al. Bone Morphogenetic Protein (BMP) signaling in development and human diseases. *Genes Dis.* **2014**, *1*, 87–105, doi:10.1016/j.gendis.2014.07.005.
23. Smith, A.; Avaron, F.; Guay, D.; Padhi, B.; Akimenko, M. Inhibition of BMP signaling during zebrafish fin regeneration disrupts fin growth and scleroblast differentiation and function. *Dev. Biol.* **2006**, *299*, 438–454, https://doi.org/10.1016/j.ydbio.2006.08.016.
24. Ho, D.M.; Whitman, M. TGF-β signaling is required for multiple processes during Xenopus tail regeneration. *Dev. Biol.* **2008**, *315*, 203–216, https://doi.org/10.1016/j.ydbio.2007.12.031.
25. Sebo, D.J.; Fetsko, A.R.; Phipps, K.K.; Taylor, M.R. Functional identification of the zebrafish Interleukin-1 receptor in an embryonic model of Il-1β-induced systemic inflammation. *Front. Immunol.* **2022**, *13*, 1039161, https://doi.org/10.3389/fimmu.2022.1039161.
26. Zhang, S.; Hu, L.; Qiao, D.; Feng, D.; Wang, H. Vacuum tribological performance of phosphonium-based ionic liquids as lubricants and lubricant additives of multialkylatedcyclopentanes. *Tribol. Int.* **2013**, *66*, 289–295. http://dx.doi.org/ 10.1016/j.triboint.2013.06.012.
27. Woods, I.G.; Wilson, C.; Friedlander, B.; Chang, P.; Reyes, D.K.; Nix, R.; Kelly, P.D.; Chu, F.; Postlethwait, J.H.; Talbot, W.S. The zebrafish gene map defines ancestral vertebrate chromosomes. *Genome Res.* **2005**, *15*, 1307–1314, https://doi.org/10.1101/gr.4134305.
28. Walczyńska, K.S.; Zhu, L.; Liang, Y. Insights into the role of the Wnt signaling pathway in the regeneration of animal model systems. *Int. J. Dev. Biol.* **2023**, *67*, 65–78, https://doi.org/10.1387/ijdb.220144yl.
29. Wehner, D.; Cizelsky, W.; Vasudevaro, M.D.; Özhan, G.; Haase, C.; Kagermeier-Schenk, B.; Röder, A.; Dorsky, R.I.; Moro, E.; Argenton, F.; et al. Wnt/β-Catenin Signaling Defines Organizing Centers that Orchestrate Growth and Differentiation of the Regenerating Zebrafish Caudal Fin. *Cell Rep.* **2014**, *6*, 467–481, https://doi.org/10.1016/j.celrep.2013.12.036.
30. Rochard, L.; Monica, S.D.; Ling, I.T.C.; Kong, Y.; Roberson, S.; Harland, R.; Halpern, M.; Liao, E.C. Roles of Wnt pathway genes *wls*, *wnt9a*, *wnt5b*, *frzb* and *gpc4* in regulating convergent-extension during palate morphogenesis. *Development* **2016**, *143*, 2541–2547, https://doi.org/10.1242/dev.137000.
31. Meng, X.-H.; Chen, B.; Zhang, J.-P. Intracellular Insulin and Impaired Autophagy in a Zebrafish model and a Cell Model of Type 2 diabetes. *Int. J. Biol. Sci.* **2017**, *13*, 985–995, https://doi.org/10.7150/ijbs.19249.
32. Zhang, Y.; Wang, L.; Zhou, W.; Wang, H.; Zhang, J.; Deng, S.; Li, W.; Li, H.; Mao, Z.; Ma, D. Tissue factor pathway inhibitor-2: A novel gene involved in zebrafish central nervous system development. *Dev. Biol.* **2013**, *381*, 38–49, https://doi.org/10.1016/j.ydbio.2013.06.018.
33. Qiu, J.-W.; Deng, M.; Cheng, Y.; Atif, R.-M.; Lin, W.-X.; Guo, L.; Li, H.; Song, Y.-Z. Sodium taurocholate cotransporting polypeptide (NTCP) deficiency: Identification of a novel *SLC10A1* mutation in two unrelated infants presenting with neonatal indirect hyperbilirubinemia and remarkable hypercholanemia. *Oncotarget* **2017**, *8*, 106598–106607, https://doi.org/10.18632/oncotarget.22503.
34. Lieber, M.R. The Mechanism of Double-Strand DNA Break Repair by the Nonhomologous DNA End-Joining Pathway. *Annu. Rev. Biochem.* **2010**, *79*, 181–211, https://doi.org/10.1146/annurev.biochem.052308.093131.
35. Kieffer, S.R.; Lowndes, N.F. Immediate-Early, Early, and Late Responses to DNA Double Stranded Breaks. *Front. Genet.* **2022**, *13*, 793884, https://doi.org/10.3389/fgene.2022.793884.
36. van de Kamp, G.; Heemskerk, T.; Kanaar, R.; Essers, J. DNA Double Strand Break Repair Pathways in Response to Different Types of Ionizing Radiation. *Front. Genet.* **2021**, *12*, https://doi.org/10.3389/fgene.2021.738230.
37. Blanpain, C.; Mohrin, M.; Sotiropoulou, P.A.; Passegué, E. DNA-Damage Response in Tissue-Specific and Cancer Stem Cells. *Cell Stem Cell* **2011**, *8*, 16–29, https://doi.org/10.1016/j.stem.2010.12.012.
38. Schnieder, J.; Mamazhakypov, A.; Birnhuber, A.; Wilhelm, J.; Kwapiszewska, G.; Ruppert, C.; Markart, P.; Wujak, L.; Rubio, K.; Barreto, G.; et al. Loss of LRP1 promotes acquisition of contractile-myofibroblast phenotype and release of active TGF-β1 from ECM stores. *Matrix Biol.* **2020**, *88*, 69–88, https://doi.org/10.1016/j.matbio.2019.12.001.
39. Andresen, C.A.; Smedegaard, S.; Sylvestersen, K.B.; Svensson, C.; Iglesias-Gato, D.; Cazzamali, G.; Nielsen, T.K.; Nielsen, M.L.; Flores-Morales, A. Protein Interaction Screening for the Ankyrin Repeats and

 doi:10.20944/preprints202604.1402.v1

Suppressor of Cytokine Signaling (SOCS) Box (ASB) Family Identify Asb11 as a Novel Endoplasmic Reticulum Resident Ubiquitin Ligase. *J. Biol. Chem.* **2014**, *289*, 2043–2054, https://doi.org/10.1074/jbc.m113.534602.

40. Wang, K.C.; Chang, H.Y. Molecular Mechanisms of Long Noncoding RNAs. *Mol. Cell* **2011**, *43*, 904–914, https://doi.org/10.1016/j.molcel.2011.08.018.
41. Martínez-Reyes, I.; Chandel, N.S. Mitochondrial TCA cycle metabolites control physiology and disease. *Nat. Commun.* **2020**, *11*, 102, https://doi.org/10.1038/s41467-019-13668-3.
42. Dreher, S.I.; Fischer, J.; Walker, T.; Diederichs, S.; Richter, W. Significance of MEF2C and RUNX3 Regulation for Endochondral Differentiation of Human Mesenchymal Progenitor Cells. *Front. Cell Dev. Biol.* **2020**, *8*, 81, https://doi.org/10.3389/fcell.2020.00081.
43. Ferrucci, V.; Lomada, S.; Wieland, T.; Zollo, M. PRUNE1 and NME/NDPK family proteins influence energy metabolism and signaling in cancer metastases. *Cancer Metastasis Rev.* **2024**, *43*, 755–775, https://doi.org/10.1007/s10555-023-10165-4.
44. Steadman, M.A.; Sumner, C.J. Changes in Neuronal Representations of Consonants in the Ascending Auditory System and Their Role in Speech Recognition. *Front. Neurosci.* **2018**, *12*, 671, https://doi.org/10.3389/fnins.2018.00671.
45. Salia, O.I.; Mitchell, D.M. Bioinformatic analysis and functional predictions of selected regeneration-associated transcripts expressed by zebrafish microglia. *BMC Genom.* **2020**, *21*, 1–17, https://doi.org/10.1186/s12864-020-07273-8.
46. Mizushima, N.; Levine, B.; Cuervo, A.M.; Klionsky, D.J. Autophagy fights disease through cellular selfdigestion. *Nature* **2008**, *451*, 1069–1075, doi:10.1038/nature06639.
47. Levine, B.; Kroemer, G. Biological Functions of Autophagy Genes: A Disease Perspective. *Cell* **2019**, *176*, 11–42, https://doi.org/10.1016/j.cell.2018.09.048.
48. Saftig P, Puertollano R. Lysosomes and their role in cellular signaling and metabolism. Nature Reviews Molecular Cell Biology. 2021;22: 503–521.
49. Klionsky, D.J.; Petroni, G.; Amaravadi, R.K.; Baehrecke, E.H.; Ballabio, A.; Boya, P.; Pedro, J.M.B.; Cadwell, K.; Cecconi, F.; Choi, A.M.K.; et al. Autophagy in major human diseases. *EMBO J.* **2021**, *40*, e108863, https://doi.org/10.15252/embj.2021108863.
50. Geiger, B.; Yamada, K.M. Molecular Architecture and Function of Matrix Adhesions. *Cold Spring Harb. Perspect. Biol.* **2011**, *3*, a005033–a005033, https://doi.org/10.1101/cshperspect.a005033.
51. Zhang, S.; Dong, Y.; Qiang, R.; Zhang, Y.; Zhang, X.; Chen, Y.; Jiang, P.; Ma, X.; Wu, L.; Ai, J.; et al. Corrigendum: Characterization of Strip1 expression in mouse cochlear hair cells. *Front. Genet.* **2024**, *15*, 1538016, https://doi.org/10.3389/fgene.2024.1538016.
52. Pahi, Z.; Borsos, B.N.; Vedelek, B.; Shidlovskii, Y.V.; Georgieva, S.G.; Boros, I.M.; Pankotai, T. TAF10 and TAF10b partially redundant roles during*Drosophila melanogaster*morphogenesis. *Transcription* **2017**, *8*, 297–306, https://doi.org/10.1080/21541264.2017.1327836.
53. Hynes, R.O. The Extracellular Matrix: Not Just Pretty Fibrils. *Science* **2009**, *326*, 1216–1219, doi:10.1126/science.1176009.
54. Kadler KE, Baldock C, Bella J, Boot-Handford RP. Collagens: Structure, function, and biosynthesis. The Journal of Cell Science. 2007;120: 1955–1958.
55. Ortinau LC, Wang H, Lei K. Identification of functionally distinct mesenchymal stem cell subsets through single-cell RNA sequencing. Developmental Cell. 2019;51: 399–413.
56. Li, H.; Wang, Z.; Liang, H.; Liu, X.; Liu, H.; Zhuang, Z.; Hou, J. Depletion of PHLDB2 Suppresses Epithelial–Mesenchymal Transition and Enhances Anti-Tumor Immunity in Head and Neck Squamous Cell Carcinoma. *Biomolecules* **2024**, *14*, 232, https://doi.org/10.3390/biom14020232.
57. Dong, H.; Zhang, P.; Song, I.; Petralia, R.S.; Liao, D.; Huganir, R.L. Characterization of the Glutamate Receptor-Interacting Proteins GRIP1 and GRIP2. *J. Neurosci.* **1999**, *19*, 6930–6941, https://doi.org/10.1523/jneurosci.19-16-06930.1999.
58. Chen, K.; Pu, L.; Hui, Y. Pivotal Role of FBXW4 in Glioma Progression and Prognosis. *Genet. Res.* **2024**, *2024*, 3005195, https://doi.org/10.1155/2024/3005195.

 doi:10.20944/preprints202604.1402.v1

59. Leiba, J.; Özbilgiç, R.; Hernández, L.; Demou, M.; Lutfalla, G.; Yatime, L.; Nguyen-Chi, M. Molecular Actors of Inflammation and Their Signaling Pathways: Mechanistic Insights from Zebrafish. *Biology* **2023**, *12*, 153, https://doi.org/10.3390/biology12020153.
60. Guo, J.; Huang, X.; Dou, L.; Yan, M.; Shen, T.; Tang, W.; Li, J. Aging and aging-related diseases: from molecular mechanisms to interventions and treatments. *Signal Transduct. Target. Ther.* **2022**, *7*, 1–40, https://doi.org/10.1038/s41392-022-01251-0.
61. Klemm, S.L.; Shipony, Z.; Greenleaf, W.J. Chromatin accessibility and the regulatory epigenome. *Nat. Rev. Genet.* **2019**, *20*, 207–220, https://doi.org/10.1038/s41576-018-0089-8.
62. Dakal, T.C.; Xiao, F.; Bhusal, C.K.; Sabapathy, P.C.; Segal, R.; Chen, J.; Bai, X. Lipids dysregulation in diseases: core concepts, targets and treatment strategies. *Lipids Heal. Dis.* **2025**, *24*, 1–21, https://doi.org/10.1186/s12944-024-02425-1.
63. Mayorca-Guiliani, A.E.; Leeming, D.J.; Henriksen, K.; Mortensen, J.H.; Nielsen, S.H.; Anstee, Q.M.; Sanyal, A.J.; Karsdal, M.A.; Schuppan, D. ECM formation and degradation during fibrosis, repair, and regeneration. *npj Metab. Heal. Dis.* **2025**, *3*, 1–17, https://doi.org/10.1038/s44324-025-00063-4.
64. Keyel, P.A. Dnases in health and disease. *Dev. Biol.* **2017**, *429*, 1–11, https://doi.org/10.1016/j.ydbio.2017.06.028.
65. Valle, F.M.; Balada, E.; Ordi-Ros, J.; Vilardell-Tarres, M. DNase 1 and systemic lupus erythematosus. *Autoimmun. Rev.* **2008**, *7*, 359–363, https://doi.org/10.1016/j.autrev.2008.02.002.
66. Jentzsch, J.; Wunderlich, H.; Thein, M.; Bechthold, J.; Brehm, L.; Krauss, S.W.; Weiss, M.; Ersfeld, K. Microtubule polyglutamylation is an essential regulator of cytoskeletal integrity in *Trypanosoma brucei*. *J. Cell Sci.* **2024**, *137*, https://doi.org/10.1242/jcs.261740.
67. Genova, M.; Grycova, L.; Puttrich, V.; Magiera, M.M.; Lansky, Z.; Janke, C.; Braun, M. Tubulin polyglutamylation differentially regulates microtubule-interacting proteins. *EMBO J.* **2023**, *42*, e112101, https://doi.org/10.15252/embj.2022112101.
68. Liu, J.; Xiao, Q.; Xiao, J.; Niu, C.; Li, Y.; Zhang, X.; Zhou, Z.; Shu, G.; Yin, G. Wnt/β-catenin signalling: function, biological mechanisms, and therapeutic opportunities. *Signal Transduct. Target. Ther.* **2022**, *7*, 1–23, https://doi.org/10.1038/s41392-021-00762-6.
69. Nair, A.; Chauhan, P.; Saha, B.; Kubatzky, K.F. Conceptual Evolution of Cell Signaling. *Int. J. Mol. Sci.* **2019**, *20*, 3292, https://doi.org/10.3390/ijms20133292.
70. Howe K. The complete sequence of the zebrafish (Danio rerio) mitochondrial genome and evolutionary patterns in vertebrate mitochondrial DNA. Genome Res. 2001;496: 1958–1967.
71. Seifert, A.W.; Duncan, E.M.; Zayas, R.M. Enduring questions in regenerative biology and the search for answers. *Commun. Biol.* **2023**, *6*, 1–13, https://doi.org/10.1038/s42003-023-05505-7.
72. Fernández-Guarino, M.; Hernández-Bule, M.L.; Bacci, S. Cellular and Molecular Processes in Wound Healing. *Biomedicines* **2023**, *11*, 2526, https://doi.org/10.3390/biomedicines11092526.
73. Xia, H.; Li, X.; Gao, W.; Fu, X.; Fang, R.H.; Zhang, L.; Zhang, K. Tissue repair and regeneration with endogenous stem cells. *Nat. Rev. Mater.* **2018**, *3*, 174–193, https://doi.org/10.1038/s41578-018-0027-6.
74. Echeverri, K.; Zayas, R.M. Regeneration: From cells to tissues to organisms. *Dev. Biol.* **2017**, *433*, 109–110, https://doi.org/10.1016/j.ydbio.2017.12.005.
75. Jin, Y.; Li, S.; Yu, Q.; Chen, T.; Liu, D. Application of stem cells in regeneration medicine. *Medcomm* **2023**, *4*, e291, https://doi.org/10.1002/mco2.291.
76. Han, P.-F.; Che, X.-D.; Li, H.-Z.; Gao, Y.-Y.; Wei, X.-C.; Li, P.-C. Annexin A1 involved in the regulation of inflammation and cell signaling pathways. *Chin. J. Traumatol.* **2020**, *23*, 96–101, https://doi.org/10.1016/j.cjtee.2020.02.002.
77. Kaina, B. A genome-wide screening for DNA repair genes: much more players than hitherto known. *Signal Transduct. Target. Ther.* **2020**, *5*, 1–2, https://doi.org/10.1038/s41392-020-00314-4.
78. Taylor, D.J.; Chhetri, S.B.; Tassia, M.G.; Biddanda, A.; Yan, S.M.; Wojcik, G.L.; Battle, A.; McCoy, R.C. Sources of gene expression variation in a globally diverse human cohort. *Nature* **2024**, *632*, 122–130, https://doi.org/10.1038/s41586-024-07708-2.
79. Katsuyama, T.; Paro, R. Epigenetic reprogramming during tissue regeneration. *FEBS Lett.* **2011**, *585*, 1617–1624, https://doi.org/10.1016/j.febslet.2011.05.010.

 doi:10.20944/preprints202604.1402.v1

80. Naba, A. Mechanisms of assembly and remodelling of the extracellular matrix. *Nat. Rev. Mol. Cell Biol.* **2024**, *25*, 865–885, https://doi.org/10.1038/s41580-024-00767-3.
81. Xu, F.; Flowers, S.; Moran, E. Essential Role of ARID2 Protein-containing SWI/SNF Complex in Tissue-specific Gene Expression. *J. Biol. Chem.* **2012**, *287*, 5033–5041, https://doi.org/10.1074/jbc.m111.279968.
82. Saghizadeh, M.; Gribanova, Y.; Akhmedov, N.B.; Farber, D.B. ZBED4, a cone and Müller cell protein in human retina, has a different cellular expression in mouse. **2011**, *17*, 2011–2018.
83. Ji, Q.; Guo, S.; Wang, X.; Pang, C.; Zhan, Y.; Chen, Y.; An, H. Recent advances in TMEM16A: Structure, function, and disease. *J. Cell. Physiol.* **2018**, *234*, 7856–7873, https://doi.org/10.1002/jcp.27865.
84. Montenegro, J.D. Gene co-expression network analysis. Methods Mol Biol. 2022;2443: 387–404. doi:10.1007/978-1-0716-2067-0_19
85. You, J.; Liu, M.; Li, M.; Zhai, S.; Quni, S.; Zhang, L.; Liu, X.; Jia, K.; Zhang, Y.; Zhou, Y. The Role of HIF-1α in Bone Regeneration: A New Direction and Challenge in Bone Tissue Engineering. *Int. J. Mol. Sci.* **2023**, *24*, 8029, https://doi.org/10.3390/ijms24098029.
86. Banu, S.; Gaur, N.; Nair, S.; Ravikrishnan, T.; Khan, S.; Mani, S.; Bharathi, S.; Mandal, K.; Kuram, N.A.; Vuppaladadium, S.; et al. Understanding the complexity of epimorphic regeneration in zebrafish caudal fin tissue: A transcriptomic and proteomic approach. *Genomics* **2022**, *114*, https://doi.org/10.1016/j.ygeno.2022.110300.
87. Akimenko, M.-A.; Johnson, S.L.; Westerfield, M.; Ekker, M. Differential induction of four *msx* homeobox genes during fin development and regeneration in zebrafish. *Development* **1995**, *121*, 347–357, https://doi.org/10.1242/dev.121.2.347.
88. Rabinowitz, J.S.; Robitaille, A.M.; Wang, Y.; Ray, C.A.; Thummel, R.; Gu, H.; Djukovic, D.; Raftery, D.; Berndt, J.D.; Moon, R.T. Transcriptomic, proteomic, and metabolomic landscape of positional memory in the caudal fin of zebrafish. *Proc. Natl. Acad. Sci.* **2017**, *114*, E717–E726, https://doi.org/10.1073/pnas.1620755114.
89. Bolger, A.M.; Lohse, M.; Usadel, B. Trimmomatic: A flexible trimmer for Illumina sequence data. *Bioinformatics* **2014**, *30*, 2114–2120. https://doi.org/10.1093/bioinformatics/btu170.
90. Kim, D.; Langmead, B.; Salzberg, S.L. HISAT: A fast spliced aligner with low memory requirements. *Nat. Methods* **2015**, *12*, 357–360, doi:10.1038/nmeth.3317.
91. Pertea, M.; Pertea, G.M.; Antonescu, C.M.; Chang, T.-C.; Mendell, J.T.; Salzberg, S.L. StringTie enables improved reconstruction of a transcriptome from RNA-seq reads. *Nat. Biotechnol.* **2015**, *33*, 290–295, https://doi.org/10.1038/nbt.3122.
92. Wucher, V.; Legeai, F.; Hédan, B.; Rizk, G.; Lagoutte, L.; Leeb, T.; Jagannathan, V.; Cadieu, E.; David, A.; Lohi, H.; et al. FEELnc: a tool for long non-coding RNA annotation and its application to the dog transcriptome. *Nucleic Acids Res.* **2017**, *45*, e57–e57, https://doi.org/10.1093/nar/gkw1306.
93. Siepel, A.; Haussler, D. Computational identification of evolutionarily conserved exons. Proceedings of the eighth annual international conference on Computational molecular biology - RECOMB '04. New York, New York, USA: ACM Press; 2004. doi:10.1145/974614.974638
94. Langfelder, P.; Horvath, S. WGCNA: an R package for weighted correlation network analysis. *BMC Bioinform.* **2008**, *9*, 559, https://doi.org/10.1186/1471-2105-9-559.
95. Yu, G.; Wang, L.-G.; Han, Y.; He, Q.-Y. clusterProfiler: An R Package for Comparing Biological Themes Among Gene Clusters. *OMICS J. Integr. Biol.* **2012**, *16*, 284–287, doi:10.1089/omi.2011.0118.
96. Uemoto, T.; Abe, G.; Tamura, K. Regrowth of zebrafish caudal fin regeneration is determined by the amputated length. *Sci. Rep.* **2020**, *10*, 1–11, https://doi.org/10.1038/s41598-020-57533-6.
97. Srivastava, P.P.; Bhasin, S.; Shankaran, S.S.; Roger, C.; Ramachandran, R.; Minocha, S. A reproducible method to study traumatic injury-induced zebrafish brain regeneration. *Biol. Methods Protoc.* **2024**, *9*, bpae073, https://doi.org/10.1093/biomethods/bpae073.